

EMBEDDED MINIMAL SURFACES OF FINITE TOPOLOGY AND ONE END

by
Christine Breiner

A dissertation submitted to Johns Hopkins University in conformity with the
requirements for the degree of Doctor of Philosophy.

Baltimore, Maryland
April, 2009

© 2009 Christine Breiner
All Rights Reserved

Abstract

In this thesis, we discuss results on complete embedded minimal surfaces in \mathbb{R}^3 with finite topology and one end. Using the tools developed by Colding and Minicozzi in their lamination theory [4, 9, 10, 11, 12], we provide a proof of the uniqueness of the helicoid. We then extend these techniques to show that any complete, embedded minimal surface with one end and finite topology is conformal to a once-punctured compact Riemann surface. Moreover, using the conformality and embeddedness, we examine the Weierstrass data and conclude that every such surface has Weierstrass data asymptotic to that of the helicoid. Using a result of Hauswirth, Perez, and Romon [19], as an immediate corollary we get that these surfaces are actually asymptotic to a helicoid (in a C^0 sense). In the final chapter, we move away from complete surfaces and consider local results on embedded disks. We sharpen results of Colding and Minicozzi on the shapes of embedded minimal disks in \mathbb{R}^3 , giving a more precise scale on which minimal disks are “helicoidal”.

READERS: William P. Minicozzi II (Advisor), Joel Spruck, Chikako Mese, Tobias Colding, and David Yarkony.

Acknowledgments

I would first like to thank my advisor, Bill Minicozzi, for providing consistent support, direction, and encouragement during a challenging time. Your dedication to me and my work made this project possible.

There are many other people at Johns Hopkins who have contributed to my success. Specifically, I would like to thank Joel Spruck and Chika Mese for being great teachers and for expecting the best from me. I thank Mike, Sid, and Susama for making the office a fun place to work. Thanks to those who came before me, who listened to me whine: Giuseppe, Brian, and Ann. And a special thanks to Hamid, for listening, encouraging, and making me laugh these last five years. You've made my life brighter. Outside of Hopkins, there are many more who deserve my thanks.

I thank my brother and sister, for loving, caring, listening, and laughing. I thank Jacob Bernstein for being such a great collaborator and friend. And I add to that important list Allison, Lori, Sarah, Laura, Sandra, Lisa, and Kate. Each of you has carried me at different times and in different ways. You all helped make this possible.

Finally, I dedicate this dissertation to my parents, who encouraged me to pursue seemingly illogical dreams. I admire the way both of you live your lives and hope to emulate your passion for life and dedication to family.

Contents

Abstract	ii
Acknowledgments	iii
List of Figures	viii
1 Introduction	1
1.1 Conformality Results on Minimal Surfaces	1
1.2 Idea of the Proof	5
1.2.1 Simply Connected Case	5
1.2.2 Non-trivial Genus Case	6
1.3 The Shapes of Minimal Disks	8
2 Background	10
2.1 Minimal Surfaces - First and Second Variation Formulas	10
2.1.1 First Variation and the Minimal Surface Equation	10
2.1.2 Second Variation and Stability	12
2.2 Multivalued Graphs and Separation	14

2.3	Weierstrass Representation	17
2.4	One Sided Curvature Estimates of Colding and Minicozzi	18
2.5	Compactness Results for Minimal Surfaces with Bounded Curvature	20
2.6	Colding-Minicozzi Lamination Theory	21
3	Uniqueness of the Helicoid	23
3.1	Preliminaries	25
3.1.1	Initial Sheets	26
3.1.2	Blow-up Pairs	33
3.2	Asymptotic Helicoids	35
3.3	Decomposition of Σ	37
3.4	Conformal Structure of Σ	40
3.4.1	Structure of f	41
3.4.2	Concluding Uniqueness	44
4	Conformal Structure of Minimal Surfaces with Finite Topology	45
4.1	Decomposition of Σ	46
4.1.1	Preliminaries	47
4.1.2	Topological structure of Σ	47
4.1.3	Rescalings of Σ	48
4.1.4	Structural Results	50
4.1.5	One-sided Curvature in Σ	53
4.1.6	Geometric Bounds Near Blow-up Pairs	54

4.1.7	Blow-up Sheets	55
4.1.8	Blow-Up Pairs	56
4.1.9	Decomposing Σ	59
4.2	Conformal Structure of Γ	62
4.2.1	Existence of f	62
4.2.2	Concluding properness of z	66
4.2.3	Conformal Structure of Σ	66
5	Local Results on Minimal Disks	68
5.1	Minimal Disks Close to a Helicoid	69
5.2	Distortions of the Helicoid	71
	Curriculum Vitae	81

List of Figures

1.1	Decomposition of Σ	7
1.2	Meeks-Weber distortion	9
2.1	The one-sided curvature estimate	18
2.2	The one-sided curvature estimate in a cone	19
4.1	Level curve examples in Proposition 4.2.2	64
5.1	Colding-Minicozzi distorted helicoids	72
5.2	The points p_i and u_i	75

Chapter 1

Introduction

1.1 Conformality Results on Minimal Surfaces

Minimal surfaces are defined as immersed surfaces that are critical points for the area functional. Using the so called first variation formula, one can easily show that every minimal surface has mean curvature identically zero. A subclass of such surfaces, area minimizing surfaces, satisfy the natural property of being the surface with least area given a prescribed boundary. There are an abundance of non-trivial examples that exist in \mathbb{R}^3 , even when one imposes the additional condition of embeddedness (i.e. without self-intersection). Classic examples of embedded minimal surfaces include the plane, catenoid, and helicoid. All three of these surfaces are planar domains, though the plane and helicoid are both embeddings of a disk, while the catenoid is an embedding of an annulus. The helicoid is often thought of as a “double spiral staircase,” and it occurs naturally (albeit with boundary) as an approximation of the

shape of DNA.

Definition 1.1.1. We define a surface to have *finite topology* if it is homeomorphic to a compact Riemann surface with a finite number of points removed.

The helicoid is a complete, embedded minimal surface with finite topology but infinite total curvature. Discovered by Meusnier in 1776, until recently the helicoid was thought to be the only complete, properly embedded minimal surface with finite topology and infinite total curvature. Work by Collin [14] established that if such a surface existed, it must have exactly one end. The discovery of a “genus-one helicoid” by Hoffman, Karcher, and Wei in 1993, [20], provided an immersed example of such a surface. In 2004, Hoffman, Weber, and Wolf [22], using a different strategy, confirmed the existence of an embedded example.

Questions of existence and uniqueness abound in the study of minimal surface theory. With the help of a compactness result of Colding and Minicozzi [12], Meeks and Rosenberg resolved a long standing question usually referred to as the *uniqueness of the helicoid* [27].

Theorem 1.1.2. (*Theorem 0.1 [27], Theorem 1.2 [2]*) *If Σ is a complete, embedded minimal disk in \mathbb{R}^3 then it is either the plane or the helicoid.*

Remark 1.1.3. The initial statement of this theorem in [27] includes the added condition that Σ be a proper embedding. Colding and Minicozzi, in [13], prove that any complete, embedded minimal surface of finite topology in \mathbb{R}^3 is automatically properly embedded. Therefore, we remove the assumption of properness from the statement of this theorem and Theorem 1.1.4 below.

The question of uniqueness for the genus-one example remains open, even when one imposes additional hypotheses in the form of strong symmetry conditions. Hoffman and White provide a variational construction of a genus-one helicoid in [25], but whether it is the same surface as the one in [22] remains unknown. A stronger understanding of the conformal structure of such surfaces appears to be a natural first step toward establishing (or refuting) uniqueness. In fact, the uniqueness of the helicoid follows almost immediately, once one establishes the minimal disk is conformal to \mathbb{C} . Previous results on the conformal structure of embedded minimal surfaces with finite topology can be found in [28] [30]. In both cases, the surfaces of interest have the added hypotheses of either more than one end or finite total curvature. The main point of this thesis is to establish a conformality result for embedded minimal surface with finite topology and one end (which are shown to have infinite total curvature).

Theorem 1.1.4. *(Theorem 1.1 in [1]) Let Σ be a complete (non-flat) minimal surface, embedded in \mathbb{R}^3 , with one end and finite topology. Then Σ is conformally a once punctured, compact Riemann surface. Moreover, the height differential, dh , extends meromorphically over the puncture with a double pole, as does the meromorphic one form $\frac{dg}{g}$.*

In the chapter that follows, we will discuss the function $g : \Sigma \rightarrow \mathbb{C}$, the stereographic projection of the Gauss map. For now, we note that the one form $\frac{dg}{g}$ has a double pole at the puncture when g has an essential singularity there. This will ultimately correspond to infinite total curvature on the surface.

Definition 1.1.5. Throughout this thesis, let $\mathcal{E}(1)$ denote the set of all complete,

embedded minimal surfaces of finite topology and one end in \mathbb{R}^3 .

For $\Sigma \in \mathcal{E}(1)$, Theorem 1.1.4, the Weierstrass representation, and embeddedness imply that near the puncture the Weierstrass data is asymptotic to that of a helicoid.

Corollary 1.1.6. *There exists an $\alpha \in \mathbb{R}$ so (for our non-flat $\Sigma \in \mathcal{E}(1)$) $\frac{dg}{g} - i\alpha dh$ has holomorphic extension over the puncture, with a zero at the puncture. Equivalently, after possibly translating parallel to the x_3 -axis, in an appropriately chosen neighborhood of the puncture, Γ , $g(p) = \exp(i\alpha z(p) + F(p))$ where $F : \Gamma \rightarrow \mathbb{C}$ extends holomorphically over the puncture with a zero there and $z = x_3 + ix_3^*$ is a holomorphic coordinate on Γ . (Here x_3^* is the harmonic conjugate of x_3 and is well defined in Γ .)*

As a consequence of this we may appeal to [19] where the behavior of annular ends with this type of Weierstrass data are studied. In particular, Hauswirth, Perez and Romon show that such an end is C^0 -asymptotic* to a (vertical) helicoid H as long as the data satisfies a certain flux condition. In the present situation, as the data is actually defined on a once punctured compact surface, this condition is automatically satisfied by Stokes' theorem and hence:

Corollary 1.1.7. *If $\Sigma \in \mathcal{E}(1)$ is non-flat then Σ is C^0 -asymptotic to some helicoid.*

Both constructions of embedded, genus-one helicoids ([22, 25]) were independently shown to have this asymptotic property. Our conformality result shows that this property is actually a necessity.

*i.e. for any $\epsilon > 0$ there exists $R_\epsilon > 0$ so that the part of the end outside of $B_{R_\epsilon}(0)$ has Hausdorff distance to H less than ϵ

1.2 Idea of the Proof

1.2.1 Simply Connected Case

The proof relies heavily on the new estimates and structural results developed by Colding and Minicozzi [4, 9, 10, 11, 12]. We first outline the argument used to provide an alternative proof of the uniqueness of the helicoid, which we detail in Chapter 3. We then explain how the introduction of the genus complicates matters slightly and changes the proof.

In Chapter 3, we show that any complete, non-flat, properly embedded minimal disk can be decomposed into two regions: one a region of strict spiraling, i.e. the union of two strictly spiraling multi-valued graphs, and the other a neighborhood of the axis along which the graphs are glued and where the normal is nearly orthogonal to the axis. This follows from existence results for multi-valued minimal graphs in embedded disks found in [10] and an approximation result for such minimal graphs from [8]. The strict spiraling is then used to see that $\nabla_{\Sigma}x_3 \neq 0$ everywhere on the surface; thus, the Gauss map is not vertical and the holomorphic map $z = x_3 + ix_3^*$ is a holomorphic coordinate. By looking at the log of the stereographic projection of the Gauss map, the strict spiraling is used to show that z is actually a proper map and thus, conformally the surface is the plane. Finally, this gives strong rigidity for the Weierstrass data implying the surface is a helicoid.

1.2.2 Non-trivial Genus Case

For $\Sigma \in \mathcal{E}(1)$, as there is finite genus, the topology of Σ is concentrated in a ball in \mathbb{R}^3 , and so by the maximum principle, all components of the intersection of Σ with a ball disjoint from the genus are disks. Hence, outside of a large ball, one may use the local results of [9, 10, 11, 12] about embedded minimal disks. In the simply connected case, the trivial topology of Σ allows one to deduce global geometric structure immediately from these local results. For $\Sigma \in \mathcal{E}(1)$, the presence of non-zero genus complicates matters. Nevertheless, the global structure will follow from the far reaching description of embedded minimal surfaces given by Colding and Minicozzi in [4]. In particular, as Σ has one end, globally it looks like a helicoid. Following the case for disks, in Chapter 4 we prove a sharper description of the global structure; indeed, one may generalize the decomposition for disks to $\Sigma \in \mathcal{E}(1)$ as:

Theorem 1.2.1. *There exist $\epsilon_0 > 0$ and \mathcal{R}_A , \mathcal{R}_S , and \mathcal{R}_G , disjoint subsets of Σ , such that $\Sigma = \mathcal{R}_A \cup \mathcal{R}_S \cup \mathcal{R}_G$. The set \mathcal{R}_G is compact, connected, has connected boundary and $\Sigma \setminus \mathcal{R}_G$ has genus 0. \mathcal{R}_S can be written as the union of two (oppositely oriented) multi-valued graphs u^1 and u^2 with $u_\theta^i \neq 0$. Finally, (after a rotation of \mathbb{R}^3) $|\nabla_\Sigma x_3| \geq \epsilon_0$ in \mathcal{R}_A .*

See Figure 1.1 for a cross section of the three regions in the decomposition of Σ as outlined in Theorem 1.2.1.

Remark 1.2.2. Here u^i multi-valued means that it can be decomposed into N -valued ϵ -sheets (see Definition 3.1.2) with varying center. The angular derivative, $(u_i)_\theta$, is

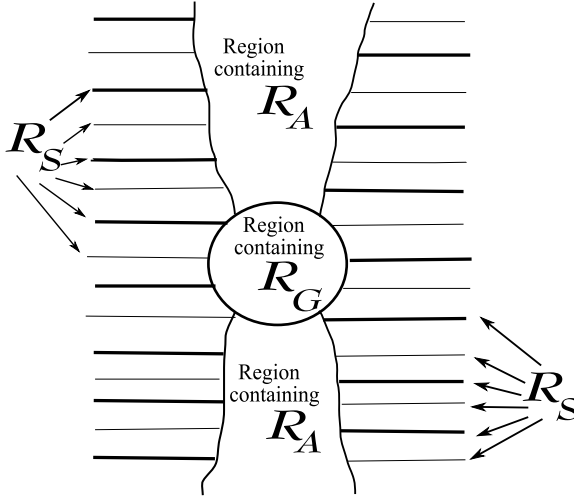


Figure 1.1: Decomposition of Σ

then with respect to the obvious polar form on each of these sheets. For simplicity we will assume throughout that both u^i are ∞ -valued.

As an important step in establishing the decomposition theorem, notice that the minimal annulus $\Gamma = \Sigma \setminus \mathcal{R}_G$ has exactly the same weak asymptotic properties as an embedded non-flat minimal disk. Thus, for both the simply connected and the non-trivial genus case, strict spiraling in \mathcal{R}_S and a lower bound for $|\nabla_{\Sigma} x_3|$ on \mathcal{R}_A together give (for appropriately chosen \mathcal{R}_G):

Proposition 1.2.3. *In Γ , $\nabla_{\Sigma} x_3 \neq 0$ and, for all $c \in \mathbb{R}$, $\Gamma \cap \{x_3 = c\}$ consists of either one smooth, properly embedded curve or two smooth, properly embedded curves each with one endpoint on $\partial\Gamma$.*

The decomposition allows us to argue as before, though the non-trivial topology again adds some technical difficulties. By Stokes' Theorem, x_3^* (the harmonic conjugate of x_3) exists on Γ and thus there is a well defined holomorphic map $z : \Gamma \rightarrow \mathbb{C}$ given by $z = x_3 + ix_3^*$. Proposition 1.2.3 implies that z is a holomorphic coordinate on

Γ . We claim that z is actually a proper map and so Γ is conformally a punctured disk. This can again be shown by studying the Gauss map. On Γ , the stereographic projection of the Gauss map, g , is a holomorphic map that avoids the origin. Moreover, the minimality of Σ and the strict spiraling in \mathcal{R}_S imply that the winding number of g around the inner boundary of Γ is zero. Hence, by monodromy there exists a holomorphic map $f : \Gamma \rightarrow \mathbb{C}$ with $g = e^f$. Then, the strict spiraling in \mathcal{R}_S imposes strong control on f which is sufficient to show that z is proper. Further, once we establish Γ is conformally a punctured disk, the properties of the level sets of f imply that it extends meromorphically over the puncture with a simple pole. This gives Theorem 1.1.4 and ultimately Corollaries 1.1.6 and 1.1.7.

1.3 The Shapes of Minimal Disks

In [9, 10, 11, 12], Colding and Minicozzi give a complete description of the structure of embedded minimal disks in a ball in \mathbb{R}^3 . Roughly speaking, they show that any such surface is either modeled on a plane (i.e. is nearly graphical) or is modeled on a helicoid (i.e. is two multi-valued graphs glued together along an axis). In the latter case, the distortion may be quite large. For instance, in [29], Meeks and Weber “bend” the helicoid; that is, they construct minimal surfaces where the axis is an arbitrary $C^{1,1}$ curve. Figure 1.2 shows cross section of one of Meeks and Weber’s examples, with the axis as a circle. We indicate a subset which is a disk. Here R is the outer scale of said disk and s the blow-up scale.

A more serious example of distortion is given by Colding and Minicozzi in [7].

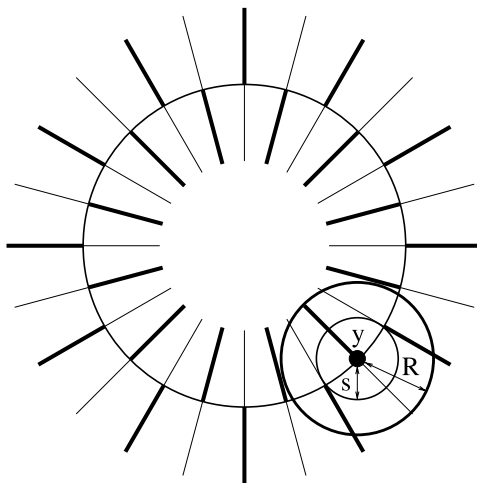


Figure 1.2: Meeks-Weber distortion

There they construct a sequence of minimal disks modeled on the helicoid, but where the ratio between the scales (a measure of the tightness of the spiraling of the multi-graphs) at different points of the axis becomes arbitrarily large. Figure 5.1 shows a cross section of one of Colding and Minicozzi's examples. Note, locally, near points of large curvature, the surface is close to a helicoid, and so the distortions are necessarily global in nature. In the final chapter of this thesis, we establish more precisely on what scale a minimal disk looks like a helicoid. (These results appear in both [2] and [3].)

Chapter 2

Background

2.1 Minimal Surfaces - First and Second Variation

Formulas

As previously mentioned, minimal surfaces are critical points for the area functional. Our work focusses solely on minimal surfaces in \mathbb{R}^3 , so we confine all definitions and consequences to this type of ambient space.

2.1.1 First Variation and the Minimal Surface Equation

When a minimal surface is graphical, it satisfies a non-linear, elliptic partial differential equation. Using the first variation formula, we can determine the appropriate PDE.

Let $u(x, y) : \Omega \subset \mathbb{R}^2 \rightarrow \mathbb{R}$ be a C^2 function. Then, an easy computation from

calculus gives that

$$Area(Graph_u) = \int_{\Omega} \sqrt{1 + |\nabla u|^2}.$$

Consider any C^1 function v such that $v|_{\partial\Omega} = 0$. We can perturb the graph of u , keeping the boundary fixed, by considering graphs of the form $u + tv$, where $t \in \mathbb{R}$.

Now, consider

$$Area(Graph_{u+tv}) = \int_{\Omega} \sqrt{1 + |\nabla(u + tv)|^2}.$$

Thus,

$$\left. \frac{d}{dt} \right|_{t=0} Area(Graph_{u+tv}) = \int_{\Omega} \frac{\langle \nabla u, \nabla v \rangle}{\sqrt{1 + |\nabla u|^2}} = - \int_{\Omega} v \operatorname{div} \left(\frac{\nabla u}{\sqrt{1 + |\nabla u|^2}} \right).$$

From this we see that u is a minimal graph, and therefore a critical point for the area functional, if and only if it satisfies

$$(2.1) \quad \operatorname{div} \left(\frac{\nabla u}{\sqrt{1 + |\nabla u|^2}} \right) = 0.$$

This is the so called *divergence form of the minimal surface equation*. Simplifying the above expression, we sometimes write it as

$$(1 + u_y^2)u_{xx} - 2u_x u_y u_{xy} + (1 + u_x^2)u_{yy} = 0.$$

Now we consider more arbitrary surfaces. Let $\Sigma \subset \mathbb{R}^3$ denote a smooth, oriented, embedded surface in \mathbb{R}^3 , possibly with boundary. As in the case for graphs, we can

locally perturb the surface through a variation. Let $\phi \in C_0^\infty(\Sigma)$ be a compactly supported smooth function on Σ . Define $\Sigma_{\phi,t} = \{x + t\phi(x)N(x) \mid x \in \Sigma\}$ where N is the unit normal to Σ . Define $A(t) = \text{Area}(\Sigma_{\phi,t})$. The first variation formula for area says that

$$(2.2) \quad \frac{dA}{dt}(0) = \int_{\Sigma} \phi H$$

where H denotes the mean curvature. That is, $H = \kappa_1 + \kappa_2$ where κ_1, κ_2 are the principle curvatures of Σ . As a consequence of (2.2), we see that Σ is minimal if and only if the mean curvature vanishes identically.

Remark 2.1.1. Note that here we have not considered variations of Σ that include a tangential direction. But, as tangential changes only correspond to a reparameterization of the surface, these have no impact on the change of area.

2.1.2 Second Variation and Stability

Of particular interest in the study of minimal surfaces are surfaces that are actually area minimizing. That is, surfaces for which $\frac{d^2}{dt^2}A(0) \geq 0$. A standard calculation for the second variation for area (see for instance section 1.7 of [5]) gives

$$(2.3) \quad \frac{d^2A}{dt^2}(0) = - \int_{\Sigma} \phi L \phi$$

where $L = \Delta_{\Sigma} + |A|^2$. Here Δ_{Σ} denotes the Laplacian intrinsically defined on Σ and $|A|^2 = \kappa_1^2 + \kappa_2^2$, the norm squared of the second fundamental form on Σ .

Definition 2.1.2. We define a minimal surface $\Sigma \subset \mathbb{R}^3$ as *stable* if $\frac{d^2 A}{dt^2}(0) \geq 0$.

By (2.3), Σ is stable if for all $\phi \in C_0^\infty(\Sigma)$, $-\int_\Sigma \phi L\phi \geq 0$. The operator L is commonly referred to as the *stability operator* or *Jacobi operator*. Notice that, using integration by parts (and the fact that ϕ is compactly supported), a minimal surface is stable iff $\int \phi^2 |A|^2 \leq \int |\nabla \phi|^2$ for all $\phi \in C_0^\infty(\Sigma)$.

We will need an important result relating stability and positive solutions to the Jacobi equation. (For proofs see [17] or [5].)

Proposition 2.1.3. *Let $\Sigma^2 \subset \mathbb{R}^3$ be an embedded minimal surface. There exists a positive function $u : \Sigma \rightarrow \mathbb{R}$ such that $Lu = 0$ iff Σ is stable.*

An important result concerning stable surfaces in \mathbb{R}^3 is the classical theorem of Bernstein:

Theorem 2.1.4. *Let $f : \mathbb{R}^2 \rightarrow \mathbb{R}$ be an entire minimal graph. Then f is affine.*

While Bernstein proved his result for entire minimal graphs, a similar result holds for complete, stable minimal immersions in \mathbb{R}^3 .

Theorem 2.1.5. *Let $\Sigma^2 \subset \mathbb{R}^3$ be a complete, orientable, stable, minimal immersion. Then Σ is a plane.*

For a proof, see [17] or [16]. Ultimately, the idea is that once a complete minimal surface is stable, one can prove quadratic area growth conditions. That is $Area(\Sigma \cap B_R) \leq CR^2$ for some fixed constant C . With quadratic area growth, one can show that Σ is actually *parabolic* (every positive superharmonic function is constant). Now the proof follows from the logic below.

Since Σ is stable, there exists $u > 0$ such that $(\Delta_\Sigma + |A|^2)u = 0$. Thus, $\Delta_\Sigma u = -|A|^2 u \leq 0$. By parabolicity, u must be constant. Thus $|A| = 0$ and Σ is flat.

We frequently use Proposition 2.1.3 and Theorem 2.1.5 to answer questions on the multiplicity of convergent surfaces. That is, if $\Sigma_i \rightarrow \Sigma_\infty$ on compact sets with multiplicity strictly greater than 1 (but finite) in \mathbb{R}^3 , then with a little care, one can construct a positive solution to the Jacobi equation and thus show that the limit surface is stable and therefore flat.

2.2 Multivalued Graphs and Separation

Throughout our work, we consider *multivalued minimal graphs*. These are modeled on the helicoid and critically, their separation also satisfies a non-linear elliptic PDE.

We denote a polar rectangle as follows:

$$(2.4) \quad S_{r_1, r_2}^{\theta_1, \theta_2} = \{(\rho, \theta) \mid r_1 \leq \rho \leq r_2, \theta_1 \leq \theta \leq \theta_2\}.$$

For a real-valued function, u , defined on a polar domain $\Omega \subset \mathbb{R}^+ \times \mathbb{R}$, define the map $\Phi_u : \Omega \rightarrow \mathbb{R}^3$ by $\Phi_u(\rho, \theta) = (\rho \cos \theta, \rho \sin \theta, u(\rho, \theta))$.

Definition 2.2.1. Given a polar domain $\Omega \subset \mathbb{R}^2$, we consider $u : \Omega \rightarrow \mathbb{R}$ to be an *N-valued graph over an annulus* if the graph of u in \mathbb{R}^3 , Γ_u , is the set $\{(\rho, \theta, u(\rho, \theta)) \mid r_1 \leq \rho \leq r_2, -N\pi \leq \theta \leq N\pi\}$.

Definition 2.2.2. We define the *separation* of the graph u by $w(\rho, \theta) = u(\rho, \theta + 2\pi) - u(\rho, \theta)$.

Thus, $\Gamma_u := \Phi_u(\Omega)$ is the graph of u , and Γ_u is embedded if and only if $w \neq 0$.

We will frequently consider multivalued graphs that satisfy the following flatness condition:

$$(2.5) \quad |\nabla u| + \rho |\text{Hess } u| + 4\rho \frac{|\nabla w|}{|w|} + \rho^2 \frac{|\text{Hess } w|}{|w|} \leq \epsilon < \frac{1}{2\pi}.$$

As an example of a multivalued graph, consider half of the helicoid. In fact, the helicoid is exactly the union of two infinite-valued graphs glued together along a singular axis. We now prove a necessary lemma concerning the difference between two minimal graphs.

Lemma 2.2.3. *Suppose that $u_1, u_2 : \Omega \rightarrow \mathbb{R}^3$ are two C^2 solutions to the minimal surface equation. Then $v = u_2 - u_1$ satisfies an equation of the form*

$$(2.6) \quad \text{div}(a_{i,j} \nabla v) = 0,$$

where the eigenvalues of $(a_{i,j})$ satisfy $0 < \nu \leq \lambda_1 \leq \lambda_2 \leq 1/\nu$. The constant ν depends on the upper bounds for the gradient of u_i .

Proof. Let $F : \mathbb{R}^2 \rightarrow \mathbb{R}^2$ under the mapping

$$F(X) = \frac{X}{(1 + |X|^2)^{1/2}}.$$

Then,

$$\begin{aligned}
0 &= F(\nabla u_2) - F(\nabla u_1) = \frac{d}{dt} \int_0^1 F(\nabla u_1 + t\nabla(u_2 - u_1)) dt \\
&= \int_0^1 dF(\nabla u_1 + t\nabla(u_2 - u_1))(\nabla(u_2 - u_1)) dt \\
&= \left(\int_0^1 dF(\nabla u_1 + t\nabla(u_2 - u_1)) dt \right) \nabla(u_2 - u_1).
\end{aligned}$$

Now we need to consider the eigenvalues of dF . First, notice that for $X, V \in \mathbb{R}^2$ with $|V| = 1$ and $X = (x_1, x_2)$, we have

$$(2.7) \quad dF(X) = \begin{pmatrix} \frac{1}{(1+|X|^2)^{1/2}} - \frac{x_1^2}{(1+|X|^2)^{3/2}} & -\frac{x_2^2}{(1+|X|^2)^{3/2}} \\ -\frac{x_1^2}{(1+|X|^2)^{3/2}} & \frac{1}{(1+|X|^2)^{1/2}} - \frac{x_2^2}{(1+|X|^2)^{3/2}} \end{pmatrix}.$$

And thus

$$(2.8) \quad dF(X)(V) = \frac{V}{(1+|X|^2)^{1/2}} - \frac{\langle X, V \rangle}{(1+|X|^2)^{3/2}} X.$$

It then follows that

$$(2.9) \quad \langle V, dF(X)(V) \rangle = \frac{(1+|X|^2) - \langle X, V \rangle^2}{(1+|X|^2)^{3/2}} \geq \frac{(1+|X|^2) - |X|^2}{(1+|X|^2)^{3/2}} \geq \frac{1}{(1+|X|^2)^{3/2}}.$$

Thus, dF is a positive definite matrix with the lower bound for its eigenvalues dependent on upper bounds for $|X|$. It follows from (2.7), that $(a_{i,j})$ is a weighted average of positive definite matrices with eigenvalues dependent on the upper bounds for $\nabla u_1, \nabla u_2$. This gives us (2.6) with the anticipated bounds on the eigenvalues of

the matrix $(a_{i,j})$. □

Note that if w is the separation of a u satisfying (2.1) and (2.5), then w satisfies a uniformly elliptic equation by Lemma 2.2.3. Thus, if Γ_u is embedded then w has pointwise gradient bounds and a Harnack inequality.

2.3 Weierstrass Representation

Individuals interested in producing new minimal surfaces frequently use Weierstrass data as a method. The Weierstrass representation takes a triple (M, g, dh) where M is a Riemann surface, g is the stereographic projection of the Gauss map, and dh is the height differential and gives an immersion into \mathbb{R}^3 . The function g is meromorphic and the one form dh has a zero everywhere g has a pole or zero. The minimal immersion in \mathbb{R}^3 is defined as

$$(2.10) \quad \mathbf{F} := \operatorname{Re} \int \left(\frac{1}{2}(g^{-1} - g), \frac{i}{2}(g^{-1} + g), 1 \right) dh.$$

Any immersed minimal surface in \mathbb{R}^3 admits such a representation.

For the helicoid with $z \in \mathbb{C}$ one has:

$$(2.11) \quad g := e^{i\alpha z}; \quad dh := dz; \quad \alpha \in \mathbb{R}.$$

Notice that on the helicoid both $\frac{dg}{g}$ and dh have double poles at infinity; moreover, $\frac{dg}{g} - i\alpha dh$ is identically zero.

2.4 One Sided Curvature Estimates of Colding and Minicozzi

The geometric decomposition theorems needed to prove both Theorem 3.0.2 and Theorem 1.1.4 rely on an important curvature estimate of Colding and Minicozzi. The idea for the theorem is quite simple; if a minimal disk comes close to but stays on one side of a plane, its curvature cannot be large.

Theorem 2.4.1. *(Theorem 0.2 of [12]) There exists $\epsilon > 0$ so that if $\Sigma \subset B_{2r_0} \cap x_3 > 0 \subset \mathbb{R}^3$ is an embedded minimal disk with $\partial\Sigma \subset \partial B_{2r_0}$, then for all components Σ' of $B_{r_0} \cap \Sigma$ which intersect $B_{\epsilon r_0}$ we have*

$$(2.12) \quad \sup_{\Sigma'} |A_\Sigma|^2 \leq r_0^{-2}.$$

See Figure 2.1 for a depiction of the estimate. The components of $\Sigma \cap B_{r_0}$ that intersect $B_{\epsilon r_0}$ are graphs.

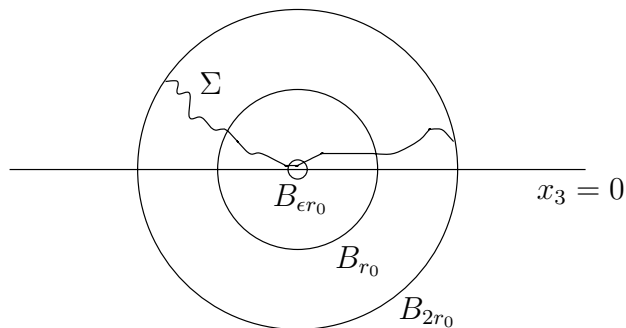


Figure 2.1: The one-sided curvature estimate

The machinery needed to determine this bound is quite complicated and required a strong understanding of the structure of embedded minimal disks with boundary

in the boundary of a ball. We frequently use a corollary to this powerful theorem, where another piece of Σ takes the place of the plane.

Corollary 2.4.2. *(Corollary I.1.9 [12]) Given $\alpha > 0$ there exists δ_0 so that the following holds:*

Let $\Sigma \subset B_{2R}$ be an embedded minimal disk with $\partial\Sigma \subset \partial B_{2R}$. If Σ contains a 2-valued graph $\Sigma_d \subset \{x_3^2 \leq \delta_0^2(x_1^2 + x_2^2)\} = \mathbf{C}_{\delta_0}$ over $D_R \setminus D_{r_0}$ with gradient $\leq \delta_0$, then each component of $B_{R/2} \cap \Sigma \setminus (\mathbf{C}_{\delta_0} \cup B_{2r_0})$ is a multivalued graph with gradient $\leq \alpha$.

See Figure 2.2. Note that Σ_d plays the role of $\{x_3 = 0\}$.

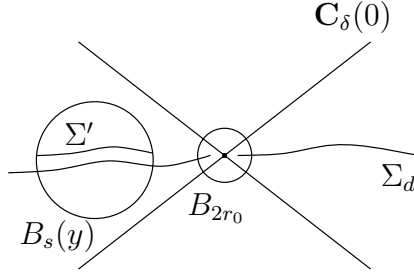


Figure 2.2: The one-sided curvature estimate in a cone

The strength of this corollary lies in the fact that one gets uniform control on the gradient of all components in the complement of a cone. In our decomposition, we find a sequence of multivalued graphs, stacked in \mathbb{R}^3 . Then, using Corollary 2.4.2, we can show that any graphs that occur between these graphs eventually (for large enough radius) have good gradient and curvature bounds.

2.5 Compactness Results for Minimal Surfaces with Bounded Curvature

Consider a surface $\Sigma^2 \subset \mathbb{R}^3$. The Gauss map is a continuous map $G : \Sigma^2 \rightarrow S^2$ such that $G(p) = N_\Sigma(p)$, where N_Σ denotes the unit normal to the surface Σ . Notice that at each point p , there are two choices for the unit normal. For an oriented minimal surface, we can globally define G after assigning one unit normal for a point $p \in \Sigma$. We sometimes refer to the second fundamental form of Σ , A , as the derivative of the Gauss map. Let E_1, E_2 be an orthonormal frame for Σ . Since, for $x \in S^2$, $N_{S^2}(x) = x$, we see that E_1, E_2 is also an orthonormal frame for S^2 . Then

$$(2.13) \quad \langle dN_{S^2}(E_i), E_j \rangle = \langle \nabla_{E_i} N, E_j \rangle = -\langle N, \nabla_{E_i} E_j \rangle = -A_{i,j}$$

where here by $A_{i,j}$ we mean the i, j component of the matrix A .

If a minimal surface has small curvature, using the fact that $|\nabla N| \leq |A|$ we can easily see that there exists some s , depending on the curvature, such that $\mathcal{B}_s(y)$ is a graph with small gradient, independent of $y \in \Sigma$. (Here $\mathcal{B}_s(y)$ denotes the intrinsic ball of radius s about y .) See for instance Lemma 2.2 in [5].

Thus, as minimal graphs satisfy an elliptic PDE (assuming gradient bounds on the graphs), we get a compactness result.

Theorem 2.5.1. *Let Σ_i be a sequence of minimal surfaces embedded in \mathbb{R}^3 . If*

$$(2.14) \quad \sup_i \sup_{K \cap \Sigma_i} |A|^2 < \infty$$

for every compact $K \subset \mathbb{R}^3$, then there exists a subsequence Σ_{i_j} and an embedded minimal surface Σ_∞ such that Σ_{i_j} converges (possibly with multiplicity) on compact sets to Σ_∞ in the C^k topology for all k .

The convergence follows immediately from the Arzela-Ascoli theorem and Schauder theory. The fact that Σ_∞ is embedded follows from the maximum principle for minimal surfaces. Also, as noted before, if Σ_∞ is nonflat, then we know the convergence is either with infinite multiplicity or with multiplicity one.

2.6 Colding-Minicozzi Lamination Theory

In a series of five papers [4, 9, 10, 11, 12], Colding and Minicozzi determine the boundary of the moduli space of complete, embedded minimal planar domains and surfaces of finite topology in \mathbb{R}^3 . We appeal to their results, both local and global, throughout this thesis. For completeness, we include here the compactness result that ultimately contains all local information.

Theorem 2.6.1. *(See Theorem 0.6 in [4].) Let $\Sigma_i \subset B_{R_i}(0) \subset \mathbb{R}^3$ be a sequence of compact, embedded minimal surfaces of fixed genus with $\partial\Sigma_i \subset \partial B_{R_i}$ and $R_i \rightarrow \infty$. If*

$$(2.15) \quad \sup_{B_1 \cap \Sigma_i} |A|^2 \rightarrow \infty$$

then there exists a subsequence Σ_j , a lamination $\mathcal{L} = \{x_3 = t\}_{t \in \mathcal{I}}$ of \mathbb{R}^3 by parallel planes (where $\mathcal{I} \subset \mathbb{R}$ is closed), and a closed non-empty set \mathcal{S} in the union of the leaves of \mathcal{L} such that, after a rotation of \mathbb{R}^3 :

1. For each $0 < \alpha < 1$, $\Sigma_j \setminus \mathcal{S}$ converges in the C^α topology to $\mathcal{L} \setminus \mathcal{S}$.
2. $\sup_{B_r(x) \cap \Sigma_j} |A|^2 \rightarrow \infty$ as $j \rightarrow \infty$ for all $r > 0$ and $x \in \mathcal{S}$. That is, the curvature blows up along \mathcal{S} .

If $\Sigma_i \in \mathcal{E}_1$ and the curvature blows up on a compact set, then one can say more about the nature of the limit. In that case, \mathcal{L} is actually a foliation of \mathbb{R}^3 by parallel planes away from a singular axis $\mathcal{S} = \mathbb{R}$, orthogonal to the leaves of \mathcal{L} . We will use the fact that \mathcal{S} consists of exactly *one* orthogonal singular axis in the proof of our decomposition, Theorem 1.2.1.

Rescalings of the helicoid (or even the genus one helicoid) provide a good illustration of the type of convergence we observe for $\Sigma_i \in \mathcal{E}(1)$. Under a sequence of rescalings, the helicoid converges to a foliation of \mathbb{R}^3 by parallel planes, away from a singular axis. The curvature blows up at every point on the axis, and all points on the axis are removable singularities of the foliation.

Chapter 3

Uniqueness of the Helicoid

In this chapter, we provide an alternative proof to the “uniqueness of the helicoid.” Most importantly, the tools developed in this chapter will be used throughout Chapter 4 to determine the conformality result, Theorem 1.1.4. Thus, the goal for this chapter is to prove the following:

Theorem 3.0.2. *The only complete, embedded minimal disks in \mathbb{R}^3 are the plane and the helicoid.*

The initial proof, given by Meeks and Rosenberg in [27], depends crucially on the lamination theory and one-sided curvature estimate of Colding and Minicozzi (see [12]). Instead of appealing to the lamination theory directly, we make use of the tools developed by Colding and Minicozzi on the existence of multivalued graphs in embedded minimal disks, as found in [9, 10, 11, 12]. Applying a result of [8] to these multivalued graphs, we approximate them by pieces of helicoids, giving explicit asymptotic behavior and geometric rigidity.

In their paper, Meeks and Rosenberg first use the lamination theory to show that (after a rotation) a homothetic blow-down of a non-flat complete, properly embedded minimal disk, Σ , is, away from some Lipschitz curve, a foliation of flat parallel planes transverse to the x_3 -axis. This gives, in a weak sense, that the surface is asymptotic to a helicoid, which they use to conclude that the Gauss map of Σ omits the north and south poles. The asymptotic structure combined with a result on parabolicity of Collin, Kusner, Meeks and Rosenberg [15], is then used to show that Σ is conformally equivalent to \mathbb{C} . Finally, they look at level sets of the log of the Gauss map and use a Picard type argument to show that this holomorphic map does not have an essential singularity at ∞ and in fact is linear. Using the Weierstrass representation, they conclude that Σ is the helicoid.

The explicit asymptotics in our paper allow for a more direct approach. We show Σ contains a central “axis” of large curvature away from which it consists of two multivalued graphs spiraling together, one strictly upward, the other downward. This is the structure of the helicoid and more generally, at least away from a compact set, the structure of the (known) embedded genus one helicoid(s) i.e. the construction of Weber, Hoffman and Wolf, [22], and that of Hoffman and White, [25], and, indeed, of any symmetric genus one helicoid (see [24]). Moreover, this is the behavior of any complete, non-flat, properly embedded minimal disk:

Theorem 3.0.3. *There exist subsets of Σ , \mathcal{R}_A and \mathcal{R}_S , with $\Sigma = \mathcal{R}_A \cup \mathcal{R}_S$ where \mathcal{R}_S can be written as the union of two (oppositely oriented) multivalued graphs u^1 and u^2 with non-vanishing angular derivative. Further, there exists $\epsilon_0 > 0$ such that on \mathcal{R}_A ,*

$$|\nabla_{\Sigma} x_3| \geq \epsilon_0.$$

Remark 3.0.4. Here u^i multivalued means that it can be decomposed into N -valued ϵ -sheets (see Definition 3.1.2) with varying center. The angular derivative is then with respect to the obvious polar form on each of these sheets. For simplicity we will assume throughout that both u^i are ∞ -valued.

In order to establish this decomposition we first use the explicit asymptotics to get the strict spiraling in \mathcal{R}_S . An application of the proof of Rado's theorem (see [30]) then gives non-vanishing of $|\nabla_{\Sigma} x_3|$ on \mathcal{R}_A and, by a Harnack inequality, the uniform lower bound. Crucially,

Proposition 3.0.5. *On Σ , $\nabla_{\Sigma} x_3 \neq 0$ and, for all $c \in \mathbb{R}$, $\Sigma \cap \{x_3 = c\}$ consists of exactly one properly embedded smooth curve.*

This implies that $z = x_3 + ix_3^*$ is a holomorphic coordinate on Σ . By looking at the stereographic projection of the Gauss map, g , in \mathcal{R}_S we show that z maps onto \mathbb{C} and so Σ is conformally the plane. This follows from the control on the behavior of g due to strict spiraling. Indeed, away from a small neighborhood of \mathcal{R}_A , Σ is conformally the union of two closed half-spaces with $\log g = f$ providing the identification. It then follows that f is also a conformal diffeomorphism which gives the uniqueness result.

3.1 Preliminaries

To study Σ we rely heavily on the structural results of Colding and Minicozzi regarding embedded minimal disks. Much of this can be found in the series of papers [9, 10, 11,

12], with more technical analysis in [6]. For a more general overview of the results, the interested reader should consult the survey [8].

Throughout this chapter, Σ will be a complete, non-flat, embedded minimal disk.

Definition 3.1.1. Let

$$(3.1) \quad \mathbf{C}_\delta(y) = \{x : (x_3 - y_3)^2 \leq \delta^2((x_1 - y_1)^2 + (x_2 - y_2)^2)\} \subset \mathbb{R}^3$$

be a cone and set $\mathbf{C}_\delta = \mathbf{C}_\delta(0)$. At some point we will need to consider such cones away from cylinders so we denote these:

$$(3.2) \quad \mathbf{C}_{\delta,R}(y) = \mathbf{C}_\delta(y) \cap \{x : (x_1 - y_1)^2 + (x_2 - y_2)^2 \geq R^2\} \subset \mathbb{R}^3.$$

3.1.1 Initial Sheets

In Colding and Minicozzi's work, multivalued minimal graphs form the basic building block used to study the structure of minimal disks. We also make heavy use of the properties of such graphs, which we normalize as follows:

Definition 3.1.2. A multivalued minimal graph Σ_0 is an N -valued (ϵ -)sheet (centered at 0 on the scale 1), if $\Sigma_0 = \Gamma_u$ and u , defined on $S_{1,\infty}^{-\pi N, \pi N}$, satisfies (2.1), (2.5), $\lim_{\rho \rightarrow \infty} \nabla u(\rho, 0) = 0$, and $\Sigma_0 \subset \mathbf{C}_\epsilon$.

Using Simons' inequality, Corollary 2.3 of [6] shows that on the one-valued middle sheet of a 2-valued graph satisfying (2.5), the Hessian of u has faster than linear decay. For an ϵ -sheet, Γ_u , this implies a Bers like result on asymptotic tangent planes. Indeed,

the normalization at ∞ gives gradient decay,

$$(3.3) \quad |\nabla u| \leq C\epsilon\rho^{-5/12}.$$

As an immediate consequence of the above, we have the following lemma:

Lemma 3.1.3. *Given $\delta > 0$ there exists an $R \geq 1$ such that if $\Sigma_0 = \Gamma_u$ is an N -valued ϵ -sheet with $N > 1$, then for Σ_0^M , the $(N - 1)$ -valued middle sheet on scale R , $\Sigma_0^M \subset \Sigma_0 \cap \mathbf{C}_{\delta,R}$.*

We now give a condition for the existence of ϵ -sheets. Roughly, all that is required is a point with large curvature relative to nearby points. Precisely,

Definition 3.1.4. The pair (y, s) , $y \in \Sigma$, $s > 0$, is a (C) *blow-up pair* if

$$(3.4) \quad \sup_{\Sigma \cap B_s(y)} |A|^2 \leq 4|A|^2(y) = 4C^2s^{-2}.$$

Having a blow-up pair forces the surface to spiral nearby (see Theorem 0.4 of [10]). In particular, after a suitable rotation we obtain an ϵ -sheet. To show that near a blow-up pair there is a single N -valued ϵ -sheet, one needs two results of Colding and Minicozzi. First, from Corollary 4.14 in [10], is the existence, near a blow-up point, of N -valued graphs that extend almost to the boundary. Then, by Proposition II.0.12 from [9], since a large number of sheets gives (2.5), after a suitable rotation one has an ϵ -sheet.

Theorem 3.1.5. *Given $\epsilon > 0$, $N \in \mathbb{Z}^+$, there exist $C_1, C_2 > 0$ so: Suppose that $(0, s)$*

is a C_1 blow-up pair of Σ . Then there exists (after a rotation of \mathbb{R}^3) an N -valued ϵ -sheet $\Sigma_0 = \Gamma_{u_0}$ on the scale s . Moreover, the separation over ∂D_s of Σ_0 is bounded below by $C_2 s$.

Proof. Proposition II.2.12 of [9] and standard elliptic estimates give an $N_\epsilon \in \mathbb{Z}^+$ and $\delta_\epsilon > 0$ so that if u satisfies (2.1) on $S_{e^{-N_\epsilon}, \infty}^{-\pi N_\epsilon, \pi N_\epsilon}$ and $\Gamma_u \subset \mathbf{C}_{\delta_\epsilon}$, then on $S_{1, \infty}^{0, 2\pi}$ we have all the terms of (2.5) bounded (by $\epsilon/2$) except $|\nabla u|$. Setting $\tau = \min\{\frac{\epsilon}{4}, \frac{\delta_\epsilon}{2}\}$ and $N_0 = N + N_\epsilon + 2$, apply Corollary 4.14 from [10] to obtain C . That is, if $(0, t)$ is a C blow-up pair, then the corollary gives an N_0 -valued graph u defined on $S_{t, \infty}^{-\pi N_0, \pi N_0}$ with $\Gamma_u \subset \mathbf{C}_\tau \cap \Sigma$ and $|\nabla u| \leq \tau$. Hence by above (and a rescaling) we see that u satisfies (2.5) on $S_{e^{N_\epsilon} t, \infty}^{-\pi N, \pi N}$. At this point we do not a priori know that $\lim_{\rho \rightarrow \infty} \nabla u(\rho, 0) = 0$. However, there is an asymptotic tangent plane. Thus after a small rotation to make this parallel to the x_1 - x_2 plane (and a small adjustment to τ and t), we may assume the limit is zero.

Proposition 4.15 of [10] gives a $\beta > 0$ so that $w(t, \theta) \geq \beta t$. Integrating (2.5), we obtain from this a C_2 so that $w(e^{N_\epsilon} t, \theta) \geq C_2 e^{N_\epsilon} t$. Finally, if we set $C_1 = C e^{N_\epsilon}$ then $(0, s)$ being a C_1 blow-up pair implies that $(0, e^{-N_\epsilon} s)$ is a C blow-up pair. This gives the result. \square

Once we have one ϵ -sheet, we can use the one-sided curvature estimates, Corollary 2.4.2, to extend the graph (and (2.5)) from an ϵ -sheet to a narrow cone. Specifically, there is a curvature bound on embedded minimal disks close to, but on one side of, a flat minimal surface. Thus, using the initial ϵ -sheet as such a flat surface implies that in an appropriately chosen cone all pieces of Σ are graphs with good estimates.

Theorem 3.1.6. *Suppose Σ contains a 4-valued ϵ -sheet Σ_0 on the scale 1 with ϵ sufficiently small. Then there exist $R \geq 1$, $\delta > 0$ depending only on ϵ such that the component of $\Sigma \cap (\mathbf{C}_\delta \setminus B_R)$ that contains the 3-valued middle sheet on scale R of Σ_0 can be expressed as the multivalued graph of a function, u , which satisfies (2.5).*

Proof. First, we establish a Harnack inequality for separation within $\mathbf{C}_{\epsilon/2,2}$. Note that the distance (as subsets of \mathbb{R}^3) between $\mathbf{C}_{\epsilon/2,2}$ and $\partial\mathbf{C}_{\epsilon,1}$ has a minimum, call it d_0 . As long as ϵ is less than δ_0 given by Corollary 2.4.2 with $\alpha = 1$, we know that the component of $\Sigma \cap \mathbf{C}_{\epsilon,1}$ containing Σ_0^M is the graph of some function u_0 defined on a polar domain Ω_0 with $|\nabla u| \leq 1$. Set $\Omega_1 = \Phi_u^{-1}(\mathbf{C}_{\epsilon/2,2})$. Then for $b \in \partial\Omega_0$ and $a \in \Omega_1$, let γ_{ab} denote a curve in Ω_0 connecting a and b normalized so $|\dot{\gamma}_{ab}| = 1$. Since intrinsic distance (in Σ) is at least as large as extrinsic distance we have

$$(3.5) \quad d_0 \leq \int_0^{\ell(\gamma_{ab})} \sqrt{1 + |\nabla u_0(\gamma_{ab}(t))|^2} dt \leq \sqrt{2}\ell(\gamma_{ab}).$$

That is, there exists a lower bound d_1 on $\text{dist}(\partial\Omega_0, \Omega_1)$ that depends only on ϵ . The separation function w is defined on smaller domains $\tilde{\Omega}_0, \tilde{\Omega}_1$. Still d_1 gives the same lower bound on $\text{dist}(\partial\tilde{\Omega}_0, \tilde{\Omega}_1)$. Thus, by the sharp Harnack inequality of [6], (using (2.6)) we have for all $x \in s\Omega_1$

$$(3.6) \quad \sup_{B_r(x)} w \leq C_H \inf_{B_r(x)} w$$

where C_H is independent of x and $r = \log(d_1/4)$.

Now given ϵ , pick N_ϵ and δ_ϵ as in the proof of Theorem 3.1.5. Set $\delta_1 = \min\{\delta_\epsilon, \epsilon/2\}$.

For $\lambda > 0$, to be chosen later, pick $\delta_2 = \delta_2(\lambda) \leq \delta_1/2$ as in Corollary 2.4.2 with $\alpha = \min\{\lambda, \epsilon/2\}$. Now pick $R_0 = R_0(\lambda)$ as in Lemma 3.1.3 using the initial sheet Σ_0 and cone \mathbf{C}_{δ_2} . Then by construction on $\Omega_2 = \Phi_u^{-1}(\mathbf{C}_{\delta_2, R_0})$, $|\nabla u| \leq \lambda$.

Integrating this gradient estimate gives $\sup_{\tilde{\Omega}_2} |w|(\rho, \theta) \leq 2\pi\lambda\rho$, where $\tilde{\Omega}_2$ is again the restriction to the subset of Ω_2 over which w is well defined. Define $N(\rho) = \lceil \frac{\theta_1^+(\rho) - \theta_2^+(\rho)}{2\pi} \rceil$, where $\theta_i^+(\rho) = \sup\{\theta \in \Gamma_i \mid (\rho, \theta) \in \Gamma_i\}$. Thus, $N(\rho)$ is approximately the number of sheets between $\partial\Omega_1$ and $\partial\Omega_2$ at a given radius. Ultimately, we want to show that $N(\rho) \geq N_\epsilon$ for all $\rho \geq R_0$. By repeated application of (3.6), with C_H adjusted to absorb r , we have

$$(3.7) \quad |w|(\rho, \theta) \leq 2\pi\lambda\rho C_H^{2\pi N(\rho)}$$

on Ω_1 . We then note

$$(3.8) \quad (\delta_1 - \delta_2)\rho \leq u_0(\rho, \theta_1^+(\rho)) - u_0(\rho, \theta_2^+(\rho)) - 2\pi N(\rho)\rho$$

$$(3.9) \quad \leq \sum_{k=1}^{N(\rho)} w(\rho, \theta_1^+(\rho) - 2\pi k)$$

$$(3.10) \quad \leq 2\pi\lambda N(\rho) C_H^{2\pi N(\rho)} \rho$$

$$(3.11) \quad \leq 2\pi C_0 \lambda C_H^{4\pi N(\rho)} \rho$$

where the last inequality comes from the fact that $xb^x \leq C_0 b^{2x}$ for C_0 depending on b . Since $\delta_2 \leq \delta_1/2$ we obtain

$$(3.12) \quad \frac{\delta_1}{4\pi\lambda} \leq C_0 C_H^{4\pi N(\rho)}.$$

Hence, by choosing λ sufficiently small, we can make $N(\rho) \geq N_\epsilon$. Finally, we pick $\delta \leq \delta_2$ and $R \geq R_0$ so that if $(\rho, \theta) \in \Omega = \Phi_u^{-1}(\mathbf{C}_{\delta,R})$ then $(e^{\pm N_\epsilon} \rho, \theta) \in \Omega_2$ and so one has (2.5) for u_0 on Ω . One can find such a δ by comparing intrinsic distance to extrinsic distance as at the beginning of the proof. \square

Remark 3.1.7. Note that all of the above results are amenable to translating and rescaling around suitable blow-up pairs given by Theorem 3.1.5.

A barrier argument then shows that there are only two such pieces. Namely, by Theorem I.0.10 of [12], the parts of Σ that lie in between an ϵ -sheet make up a second multivalued graph. Furthermore, one-sided curvature gives gradient estimates which, coupled with the estimates we get given enough sheets, reveal that this graph actually contains an ϵ -sheet. Thus, around a blow-up point, Σ consists of two ϵ -sheets spiraling together.

We now make the last statement precise. Suppose u is defined on $S_{1/2,\infty}^{-\pi N-3\pi,\pi N+3\pi}$ and Γ_u is embedded. We define E to be the region over $D_\infty \setminus D_1$ between the top and bottom sheets of the concentric subgraph of u . That is:

$$(3.13) \quad E = \{(\rho \cos \theta, \rho \sin \theta, t) : \\ 1 \leq \rho \leq \infty, -2\pi \leq \theta < 0, u(\rho, \theta - \pi N) < t < u(\rho, \theta + (N + 2)\pi)\}.$$

Using Theorem I.0.10 of [12], Theorem 3.1.5, and one-sided curvature, we have:

Theorem 3.1.8. *Given $\epsilon > 0$ sufficiently small, there exist $C_1, C_2 > 0$ so: Suppose $(0, s)$ is a C_1 blow-up pair. Then there exist two 4-valued ϵ -sheets $\Sigma_i = \Gamma_{u_i}$ ($i = 1, 2$)*

on the scale s which spiral together (i.e. $u_1(s, 0) < u_2(s, 0) < u_1(s, 2\pi)$). Moreover, the separation over ∂D_s of Σ_i is bounded below by $C_2 s$.

Remark 3.1.9. We refer to Σ_1, Σ_2 as (ϵ) -blow-up sheets associated with (y, s) .

Proof. Choose $\epsilon_0 > 0$ and N_0 as in Theorem I.0.10 (of [12]). For $\epsilon < \epsilon_0$ choose $N_\epsilon, \delta_\epsilon$ as in the proof of Theorem 3.1.5. With $N - 6 = \max\{N_\epsilon + 4, N_0\}$ denote by C'_1, C'_2 the constants given by Theorem 3.1.5. Thus, if $(0, r)$ is a C'_1 blow-up pair then there exists an N -valued ϵ -sheet $\Sigma'_1 = \Gamma_{u'_1}$ on scale r inside of Σ . Applying Theorem I.0.10 to u'_1 , we see that $\Sigma \cap E \setminus \Sigma'_1$ is given by the graph of a function u'_2 defined on $S_{2r, \infty}^{-\pi N_\epsilon - 4\pi, \pi N_\epsilon + 4\pi}$. In particular, for u'_2 on $S_{2e^{N_\epsilon} r, \infty}^{-4\pi, 4\pi}$ we have (2.5) as long as we can control $|\nabla u'_2|$. But here we use one-sided curvature (and the ϵ -sheet Σ'_1). Namely, given $\alpha = \min\{\epsilon/2, \delta_\epsilon\}$, one-sided curvature estimates allow us to choose $\delta_0 > 0$ so that in the cone \mathbf{C}_{δ_0} (and outside a ball) Σ is graphical with gradient less than α . By (3.3), there exists $r_1 > 0$ such that $|\nabla u'_1| \leq \delta_0$ on $S_{r_1, \infty}^{-5\pi, 5\pi}$ and this 5-valued graph is contained in $\mathbf{C}_{\delta_0} \setminus B_{r_1}$. Moreover, since five sheets of u'_1 are inside of \mathbf{C}_{δ_0} , the four concentric sheets of u'_2 are also in that cone. Set $\gamma = \max\{2e^{N_\epsilon}, 1\}$. Let u_1 and u_2 be given by restricting u'_1 and u'_2 to $S_{\gamma r_1, \infty}^{-4\pi, 4\pi}$ and define $\Sigma_i = \Gamma_{u_i}$.

Set $C_1 = \gamma C'_1$, so if $(0, s)$ is a C_1 blow-up pair then Σ_i will exist on scale s . Integrating (2.5), the lower bound C'_2 gives a lower bound on initial separation of Σ_1 . We find C_2 by noting that if the initial separation of Σ_2 was too small there would be two sheets between one sheet of Σ_1 . \square

3.1.2 Blow-up Pairs

Since Σ is not a plane, we can always find at least one blow-up pair (y, s) . We then use this initial pair to find a sequence of blow-up pairs forming an “axis” of large curvature. The key results we need are Lemma 5.1 of [10], which says that as long as curvature is large enough in some ball we can find a blow-up pair in the ball, and Corollary III.3.5 of [11], which guarantees points of large curvature above and below blow-up points. Colding and Minicozzi, in [13], provide a good overview of this process of decomposing Σ into blow-up sheets. The main result is the following (see Lemma 2.5 of [13]):

Theorem 3.1.10. *For $1/2 > \gamma > 0$ and $\epsilon > 0$ both sufficiently small, let C_1 be given by Theorem 3.1.8. Then there exists $C_{in} > 4$ and $\delta > 0$ so: If $(0, s)$ is a C_1 blow-up pair then there exist (y_+, s_+) and (y_-, s_-) , C_1 blow-up pairs, with $y_{\pm} \in \Sigma \cap B_{C_{in}s} \setminus (B_{2s} \cup \mathbf{C}_{\delta})$, $x_3(y_+) > 0 > x_3(y_-)$, and $s_{\pm} \leq \gamma|y_{\pm}|$.*

Hence, given a blow-up pair, we can iteratively find a sequence of blow-up pairs ordered by height and lying outside of a cone, with distance between subsequent pairs bounded by a fixed multiple of the scale.

Proof. For simplicity let us rescale so that $s = 1$. Since $(0, 1)$ is a C_1 blow-up pair, Theorem 3.1.8 gives two blow-up sheets $\Sigma_i = \Gamma_{u_i}$ ($i = 1, 2$). Let ν denote $\partial\Sigma_{0,2}$, the boundary of the component of $B_2 \cap \Sigma$ containing 0. By the maximum principle this is a simple closed curve. Since $\text{dist}(\Sigma_i, 0) < 2$, ν meets both Σ_1 and Σ_2 . Hence ν contains two curves $\nu_{\pm} \subset \Sigma \cap \partial B_2$ that connect the Σ_i above and below 0 respectively.

This is accomplished by choosing appropriate components of $\nu \setminus (\Sigma_1 \cup \Sigma_2)$. Let Σ_{\pm} be the component of $\Sigma \setminus (\Sigma_1 \cup \Sigma_2 \cup \nu_{\pm})$ that does not contain $\Sigma_{0,1}$ (again these will be above and below 0). Without loss of generality we will focus on Σ_+ (i.e above 0).

By Corollary III.3.5 of [11], for C_3 (to be chosen later) there exists C_2 depending on C_3 , and an element $x \in \Sigma_{0,C_2} \cap \Sigma_+ \setminus B_4$ with $|x|^2 |A|^2(x) \geq 4C_3^2$. Let $\delta_0 > 0$ be given by the corollary of the one-sided curvature estimates, Corollary I.1.9 of [12]. As long as $\epsilon < \delta_0$, one-sided curvature gives a C_4 so that: for $z \in \mathbf{C}_{\delta_0} \cap \Sigma \setminus B_{2s}$, $|z|^2 |A|^2 \leq 4C_4^2$. Hence choosing $C_3 \geq C_4$ forces x out of this set. Thus, $x \in \Sigma_+ \cap B_{C_2} \setminus (\mathbf{C}_{\delta_0} \cup B_4)$.

The lower bound on $\sup |x|^2 |A|^2$ implies that

$$(3.14) \quad \sup_{B_{\frac{\gamma}{2}|x|}(x)} |A|^2 \geq 16 \left(\frac{\gamma C_3}{2} \right)^2 (\gamma |x|)^{-2}.$$

Now, applying Lemma 5.1 of [10] we obtain $y \in B_{\gamma|x|}(x) \cap \Sigma$ and $r_1 \leq \gamma|x| - |y - x|$ so that (y, r_1) is a $\frac{\gamma C_3}{2}$ blow-up pair. If necessary, increase C_3 so that $\frac{\gamma C_3}{2} \geq C_1$. Then for $t = \frac{C_1}{\gamma C_3} r_1 \leq \frac{1}{2} r_1 \leq \frac{\gamma}{2} |x|$, (y, t) is a C_1 blow-up pair. Note that since $\frac{1}{2}|x| \leq (1 - \gamma)|x| \leq |y| \leq (1 + \gamma)|x|$, one has $t \leq \gamma|y|$.

The above inequalities imply that if we set $C_{in} = (1 + \gamma)C_2$ then $y \in \Sigma \cap B_{C_{in}} \setminus B_{4(1-\gamma)} \subset B_{C_{in}} \setminus B_2$. To determine δ , notice that for $\gamma \leq \frac{\delta_0}{2\sqrt{1+\delta_0^2}}$, $x_3(y) \geq \frac{1}{2}x_3(x) \geq C(\delta_0)$. Thus, for $\delta < \frac{C(\delta_0)}{C_{in}}$, $y \in \Sigma \setminus \mathbf{C}_{\delta}$. Setting $(y_+, s_+) = (y, t)$ and making the same argument for (y_-, s_-) gives the result. \square

Hence, given a blow-up pair, we can iteratively find a sequence of blow-up pairs ordered by height and lying outside of a cone, with distance between subsequent pairs

bounded by a fixed multiple of the scale.

By the lamination theory, the existence of a blow-up pair imposes strong control on nearby geometry. The chord-arc bounds and Lemma 2.26 of [13] are examples.

We also have:

Proposition 3.1.11. *Given K , there is an N so that: If (y_1, s_1) and (y_2, s_2) are C blow-up pairs of Σ with $y_2 \in B_{Ks_1}(y_1)$, then the number of sheets between the associated blow-up sheets is at most N .*

Proof. We note that for a large, universal constant C' the area of $B_{C'Ks_1}(y_1) \cap \Sigma$ gives a bound on N , so it is enough to uniformly bound this area. The chord-arc bounds of [13] give a uniform constant γ depending only on C' so that $B_{C'Ks_1}(y_1) \cap \Sigma$ is contained in $\mathcal{B}_{\gamma Ks_1}(y_1)$ the intrinsic ball in Σ of radius γKs_1 . Furthermore, Lemma 2.26 of [13] gives a uniform bound on the curvature of Σ in $\mathcal{B}_{\gamma Ks_1}(y_1)$ and hence a uniform bound on the area of $\mathcal{B}_{\gamma Ks_1}(y_1)$. Since $B_{C'Ks_1}(y_1) \cap \Sigma \subset \mathcal{B}_{\gamma Ks_1}(y_1)$ it also has uniformly bounded area. □

3.2 Asymptotic Helicoids

Lemma 14.1 of [8] and the gradient decay (3.3) shows that ϵ -sheets can be approximated by a combination of planar, helicoidal, and catenoidal pieces. Precisely, there is a “laurent expansion” for the almost holomorphic function $u_x - iu_y$. This result allows us to bound the oscillation on broken circles $C(\rho) := S_{\rho, \rho}^{-\pi, \pi}$ of u_θ , which yields asymptotic lower bounds for u_θ .

Lemma 3.2.1. *Given Γ_u , a 3-valued ϵ -sheet on scale 1, set $f = u_x - iu_y$. Then for $r_1 \geq 1$ and $\zeta = \rho e^{i\theta}$ with $(\rho, \theta) \in S_{2r_1, \infty}^{-\pi, \pi}$*

$$(3.15) \quad f(\zeta) = c\zeta^{-1} + g(\zeta)$$

where $c = c(r_1, u) \in \mathbb{C}$ and $|g(\zeta)| \leq C_0 r_1^{-1/4} |\zeta|^{-1} + C_0 \epsilon r_1^{-1} |w(r_1, -\pi)|$.

Using this approximation result we now bound the oscillation.

Lemma 3.2.2. *Suppose Γ_u is a 3-valued ϵ -sheet on scale 1. Then for $\rho \geq 2$, there exists a universal C so:*

$$(3.16) \quad \operatorname{osc}_{C(\rho)} u_\theta \leq C \rho^{-1/4} + C \epsilon |w(\rho, -\pi)|.$$

Proof. Using Lemma 3.2.1 and the identification $u_\theta(\rho, \theta) = -\operatorname{Im} \zeta f(\zeta)$ for $\zeta = \rho e^{i\theta}$, we compute:

$$\begin{aligned} \operatorname{osc}_{C(\rho)} u_\theta &= \sup_{|\zeta|=\rho} \operatorname{Im} (-c - \zeta g(\zeta)) - \inf_{|\zeta|=\rho} \operatorname{Im} (-c - \zeta g(\zeta)) \\ &\leq 2 \sup_{|\zeta|=\rho} |\zeta| |g(\zeta)| \leq 4C_0 \rho^{-1/4} + 2C_0 \epsilon |w(\rho/2, -\pi)|. \end{aligned}$$

The last inequality comes from Lemma 3.2.1, setting $2r_1 = \rho$. Finally, integrate (2.5) to get the bound $|w|(\rho/2, -\pi) \leq |w|(\rho, -\pi)$ and choose C sufficiently large. \square

Integrating u_θ around $C(\rho)$ gives $w(\rho, -\pi)$, which yields a lower bound on $\sup_{C(\rho)} u_\theta$ in terms of the separation. The oscillation bound of (3.16) then gives a lower bound for u_θ . Indeed, for ϵ sufficiently small and large ρ , u_θ is positive.

Proposition 3.2.3. *There exists an ϵ_0 so: Suppose Γ_u is a 3-valued ϵ -sheet on scale 1 with $\epsilon < \epsilon_0$ and $w(1, \theta) \geq C_2 > 0$. Then there exists $C_3 = C_3(C_2) \geq 2$, so that on $S_{C_3, \infty}^{-\pi, \pi}$:*

$$(3.17) \quad u_\theta(\rho, \theta) \geq \frac{C_2}{8\pi} \rho^{-\epsilon}.$$

Proof. Since $\int_{-\pi}^{\pi} u_\theta(\rho, \theta) d\theta = w(\rho, -\pi)$ we see $w(\rho, -\pi) \leq 2\pi \sup_{C(\rho)} u_\theta$. Using the oscillation bound (3.16) then gives the lower bound:

$$(3.18) \quad (1 - 2\pi C\epsilon)w(\rho, -\pi) - 2\pi C\rho^{-1/4} \leq 2\pi \inf_{C(\rho)} u_\theta.$$

Pick ϵ_0 so that $2\pi C\epsilon_0 \leq 1/2$. Integrating (2.5) yields $w(\rho, \theta) \geq w(1, \theta)\rho^{-\epsilon} \geq C_2\rho^{-\epsilon}$.

Thus,

$$(3.19) \quad \inf_{C(\rho)} u_\theta \geq \frac{C_2}{4\pi} \rho^{-\epsilon} - C\rho^{-1/4}.$$

Since $\epsilon < 1/4$, just choose C_3 large. □

3.3 Decomposition of Σ

In order to decompose Σ , we use the explicit asymptotic properties found above to show that, away from the “axis,” Σ consists of two strictly spiraling graphs. In particular, this implies that all intersections of Σ with planes transverse to the x_3 -axis have exactly two ends. The proof of Rado’s theorem then gives that $\nabla_{\Sigma} x_3$ is non-

vanishing and so each level set consists of one unbounded smooth curve. A curvature estimate and a Harnack inequality then give the lower bound on $|\nabla_{\Sigma} x_3|$ near the axis. To prove Theorem 3.0.3 we first construct \mathcal{R}_S .

Lemma 3.3.1. *There exist constants C_1, R_1 and a sequence (y_i, s_i) of C_1 blow-up pairs of Σ so that: $x_3(y_i) < x_3(y_{i+1})$ and for $i \geq 0$, $y_{i+1} \in B_{R_1 s_i}(y_i)$ while for $i < 0$, $y_{i-1} \in B_{R_1 s_i}(y_i)$. Moreover, if \mathcal{R}_A is the connected component of $\bigcup_i B_{R_1 s_i}(y_i) \cap \Sigma$ containing y_0 and $\mathcal{R}_S = \Sigma \setminus \mathcal{R}_A$, then \mathcal{R}_S has exactly two unbounded components, which are (oppositely oriented) multivalued graphs u^1 and u^2 with $u_{\theta}^i \neq 0$. In particular, $\nabla_{\Sigma} x_3 \neq 0$ on the two graphs.*

Proof. Fix $\epsilon < \epsilon_0$ where ϵ_0 is given by Proposition 3.2.3. Using this ϵ , from Theorem 3.1.8 we obtain the blow-up constant C_1 and denote by C_2 the lower bound on initial separation. Suppose $0 \in \Sigma$ and that $(0, 1)$ is a C_1 blow-up pair. From Theorem 3.1.10 there exists a constant C_{in} so that there are C_1 blow-up pairs (y_+, s_+) and (y_-, s_-) with $x_3(y_-) < 0 < x_3(y_+)$ and $y_{\pm} \in B_{C_{in}}$. Note by Proposition 3.1.11 that there is a fixed upper bound N on the number of sheets between the blow-up sheets associated to (y_{\pm}, s_{\pm}) and the sheets Σ_i^0 ($i = 1, 2$) associated to $(0, 1)$.

As a consequence of Theorem 3.1.6, there exists an R so that all the N sheets above and the N sheets below Σ_i^0 are ϵ -sheets centered on the x_3 -axis on scale R . Call these pairs of 1-valued sheets Σ_i^j with $-N \leq j \leq N$. Integrating (2.5), we obtain from C_2 and N a value, C'_2 , so that for all Σ_i^j , the separation over ∂D_R is bounded below by C'_2 . Non-vanishing of the right hand side of (3.17) is scaling invariant, so there exists a C_3 such that: on each Σ_i^j , outside of a cylinder centered on the x_3 -axis

of radius RC_3 , $u_\theta^i \neq 0$. The chord-arc bounds of [13] (i.e. Theorem 0.5) then allow us to pick R_1 large enough so the component of $B_{R_1} \cap \Sigma$ containing 0 contains this cylinder, the points y_+, y_- and meets each Σ_i^j . Finally, we note that all the statements in the theorem are invariant under rescaling. Hence, use Theorem 3.1.10 to construct a sequence of C_1 blow-up pairs (y_i, s_i) satisfying the necessary conditions. \square

The placement of the blow-up pairs and the strict spiraling gives:

Lemma 3.3.2. *For all h , there exist $\alpha, \rho_0 > 0$ so that for all $\rho > \rho_0$ the set $\Sigma \cap \{x_3 = c\} \cap \{x_1^2 + x_2^2 = \rho^2\}$ consists of exactly two points for $|c - h| \leq \alpha$.*

Proof. First note, for ρ_0 large, the intersection is never empty by the maximum principle and because Σ is proper. Without loss of generality we may assume $h = 0$ with $0 \in Z^0 = \Sigma \cap \{x_3 = 0\}$ and $|A|^2(0) \neq 0$. Let R_1 and the set of blow-up pairs be given by Lemma 3.3.1. There then exists ρ_0 so for $2\rho > \rho_0$, $\{x_1^2 + x_2^2 = \rho^2\} \cap Z^0$ lies in the set \mathcal{R}_S . If no such ρ_0 existed then, since the blow-up pairs lie outside a cone, there would exist $\delta > 0$ and a subset of the blow-up pairs (y_i, s_i) so $0 \in B_{\delta R_1 s_i}(y_i)$. However, Lemma 2.26 of [13], with $K_1 = \delta R_1$, would then imply $|A|^2(0) \leq K_2 s_i^{-2}$, or $|A|^2(0) = 0$, a contradiction. Now, for some small α and $\rho > \rho_0$, $Z^c \cap \{x_1^2 + x_2^2 = \rho^2\}$ lies in \mathcal{R}_S for all $|c| < \alpha$, and so $\{x_1^2 + x_2^2 = \rho^2\} \cap \{-\alpha < x_3 < \alpha\} \cap \Sigma$ consists of the union of the graphs of u^1 and u^2 over the circle ∂D_ρ , both of which are monotone increasing in height. \square

As x_3 is harmonic on Σ , Proposition 3.0.5 is an immediate consequence of the previous result. We now show Theorem 3.0.3:

Proof. By Lemma 3.3.1 it remains to show that $|\nabla_{\Sigma}x_3|$ is bounded below on \mathcal{R}_A . Suppose that $(0, 1)$ is a blow-up pair. By the chord-arc bounds of [13], there exists γ large enough so that the intrinsic ball of radius γR_1 contains $\Sigma \cap B_{R_1}$. Lemma 2.26 of [13] implies that curvature is bounded in $B_{2\gamma R_1} \cap \Sigma$ uniformly by K . The function $v = -2 \log |\nabla_{\Sigma}x_3| \geq 0$ is well defined and smooth by Proposition 3.0.5 and standard computations give $\Delta_{\Sigma}v = |A|^2$. Then, since $|\nabla_{\Sigma}x_3| = 1$ somewhere in the component of $B_1(0) \cap \Sigma$ containing 0, we can apply a Harnack inequality (see Theorems 9.20 and 9.22 in [18]) to obtain an upper bound for v on the intrinsic ball of radius γR_1 that depends only on K . Consequently, there is a lower bound ϵ_0 on $|\nabla_{\Sigma}x_3|$ in $\Sigma \cap B_{R_1}$. Since this bound is scaling invariant, the same bound holds around any blow-up pair. Finally, any bounded component, Ω , of \mathcal{R}_S has boundary in \mathcal{R}_A and so, since v is subharmonic, $|\nabla_{\Sigma}x_3| \geq \epsilon_0$ on Ω . Thus, by adjoining all such bounded Ω to \mathcal{R}_A we obtain Theorem 3.0.3. \square

3.4 Conformal Structure of Σ

Since $\nabla_{\Sigma}x_3$ is non-vanishing and the level sets of x_3 in Σ consist of a single curve, the map $z = x_3 + ix_3^* : \Sigma \rightarrow \mathbb{C}$ is a global holomorphic coordinate (here x_3^* is the harmonic conjugate of x_3). Additionally, $\nabla_{\Sigma}x_3 \neq 0$ implies that the normal of Σ avoids $(0, 0, \pm 1)$. Thus, the stereographic projection of the Gauss map, denoted by g , is a holomorphic map $g : \Sigma \rightarrow \mathbb{C} \setminus \{0\}$. By monodromy, there exists a holomorphic map $f = f_1 + if_2 : \Sigma \rightarrow \mathbb{C}$ so that $g = e^f$. We will use f to show that z is actually a conformal diffeomorphism between Σ and \mathbb{C} . As the same is then true for

f , embeddedness and the Weierstrass representation implies Σ is the helicoid.

3.4.1 Structure of f

We note the following relation between $\nabla_{\Sigma}x_3$, g and f :

$$(3.20) \quad |\nabla_{\Sigma}x_3| = 2\frac{|g|}{1+|g|^2} \leq 2e^{-|f_1|}.$$

An immediate consequence of (3.20) and the decomposition of Theorem 3.0.3 is that there exists $\gamma_0 > 0$ so on \mathcal{R}_A , $|f_1(z)| \leq \gamma_0$. This imposes strong rigidity on f :

Proposition 3.4.1. *Let $\Omega_{\pm} = \{x \in \Sigma : \pm f_1(x) \geq 2\gamma_0\}$ then f is a proper conformal diffeomorphism from Ω_{\pm} onto the closed half-spaces $\{z : \pm \operatorname{Re} z \geq 2\gamma_0\}$.*

Proof. Let $\gamma > \gamma_0$ be a regular value of f_1 . Such γ exists by Sard's theorem and indeed form a dense subset of (γ_0, ∞) . We first claim that the smooth submanifold $Z = f_1^{-1}(\gamma)$ has a finite number of components. Note that Z is non-empty by (3.3) and (3.20). By construction, Z is a subset of \mathcal{R}_S and, up to choosing an orientation, Z lies in the graph of u^1 , which we will henceforth denote as u . Let us parameterize one of the components of Z by $\phi(t)$, non-compact by the maximum principle, and write $\phi(t) = \Phi_u(\rho(t), \theta(t))$.

At the point $\Phi_u(\rho, \theta)$ we compute:

$$(3.21) \quad g(\rho, \theta) = -\frac{1}{\sqrt{1+|\nabla u|^2}-1} \left(u_{\rho}(\rho, \theta) + i\frac{u_{\theta}(\rho, \theta)}{\rho} \right) e^{i\theta}.$$

Since $u_\theta(\rho(t), \theta(t)) > 0$, there exists a function $\tilde{\theta}(t)$ with $\pi < \tilde{\theta}(t) < 2\pi$ such that

$$(3.22) \quad |\nabla u|(\rho(t), \theta(t))e^{i\tilde{\theta}(t)} = -u_\rho(\rho(t), \theta(t)) - i\frac{u_\theta(\rho(t), \theta(t))}{\rho(t)}.$$

Thus $f_2(\phi(t)) = \theta(t) + \tilde{\theta}(t)$.

We now claim $\lim_{t \rightarrow \pm\infty} |f_2(\phi(t))| = \infty$. Suppose $\lim_{t \rightarrow \infty} f_2(\phi(t)) = R < \infty$ and $f_2(\phi(t)) < R$. Then, the formula for $f_2(\phi(t))$ implies that for t large $\phi(t)$ lies in one sheet. The decay estimates (3.3) together with (3.20) imply $\rho(t)$ cannot become arbitrarily large and so the positive end of ϕ lies in a compact set. Thus, there is a sequence of points $p_j = \phi(t_j)$, with t_j monotonically increasing to ∞ , so $p_j \rightarrow p_\infty \in \Sigma$. By the continuity of f_1 , $p_\infty \in Z$, and since $f_2(p_j)$ is monotone increasing with supremum R , $f_2(p_\infty) = R$, and so p_∞ is not in ϕ . However, $p_\infty \in Z$ implies $f'(p_\infty) \neq 0$ and so f restricted to a small neighborhood of p_∞ is a diffeomorphism onto its image, contradicting ϕ coming arbitrarily close to p_∞ .

Thus, the formula for $f_2(\phi(t))$ and the bound on $\tilde{\theta}$ show that $\theta(t)$ must extend from $-\infty$ to ∞ . We now conclude that there are at most a finite number of components of Z . Namely, since $\theta(t)$ runs from $-\infty$ to ∞ we see that every component of Z must meet the curve $\eta(\rho) = \Phi_u(\rho, 0) \in \mathcal{R}_S$. Again, the gradient decay of (3.3) says that the set of intersections of Z with η lies in a compact set, and so consists of a finite number of points. Now, suppose there was more than one component of Z . Looking at the intersection of Z with η , we order these components innermost to outermost; parameterize the innermost curve by $\phi_1(t)$ and the outermost by $\phi_2(t)$. Pick τ a regular value for f_2 , and parameterize the component of $f_2^{-1}(\tau)$ that meets ϕ_1 by

$\sigma(t)$, writing $\sigma(t) = \Phi_u(\rho(t), \theta(t))$ in \mathcal{R}_S . From the formula for f_2 , $|\theta(t) - \tau| \leq 2\pi$. Again, $\sigma(t)$ cannot have an end in a compact set, so $\rho(t) \rightarrow \infty$. Hence, σ must also intersect ϕ_2 contradicting the monotonicity of f_1 on σ .

Hence, when $\gamma > \gamma_0$, is a regular value of f_1 , $f_1^{-1}(\gamma)$ is a single smooth curve. We claim this implies that all $\gamma > \gamma_0$ are regular values. Suppose $\gamma' > \gamma_0$ were a critical value of f_1 . Then, as f_1 is harmonic, the proof of Rado's theorem implies for $\gamma > \gamma_0$, a regular value of f_1 near γ' , $f_1^{-1}(\gamma)$ would have at least two components. Thus, $f : \Omega_+ \rightarrow \{z : \operatorname{Re} z \geq 2\gamma_0\}$ is a conformal diffeomorphism that maps boundaries onto boundaries, immediately implying f is also proper on Ω_+ , and similarly for Ω_- . \square

By looking at z , which already has well understood behavior away from ∞ , we see that Σ is conformal to \mathbb{C} with z providing an identification.

Proposition 3.4.2. *The map $h \circ z^{-1} : \mathbb{C} \rightarrow \mathbb{C}$ is linear.*

Proof. We first show that z is a conformal diffeomorphism between Σ and \mathbb{C} , that is z is onto. This follows if we show x_3^* goes from $-\infty$ to ∞ on the level sets of x_3 . The key fact is: each level set of x_3 has one end in Ω_+ and the other in Ω_- . This is an immediate consequence of the radial gradient decay on level sets of x_3 forced by the one-sided curvature estimate. Indeed, x_3 runs from $-\infty$ to ∞ along the curve $\partial\Omega_+$ and so $z(\partial\Omega_+)$ splits \mathbb{C} into two components with only one, V , meeting $z(\Omega_+) = U$. After conformally straightening the boundary of V (using the Riemann mapping theorem) and precomposing with $f|_{\Omega_+}^{-1}$ we obtain a map from a closed half-space into a closed half-space with the boundary mapped to the boundary. We claim that this map is necessarily onto, that is U equals \bar{V} . Suppose it was not onto, then

a Schwarz reflection would give a holomorphic map from \mathbb{C} into a simply connected proper subset of \mathbb{C} . Because the latter is conformally a disk, Liouville's theorem would imply this map was constant, a contradiction. As a consequence, if $p \rightarrow \infty$ in Ω_+ then $z(p) \rightarrow \infty$, with the same true in Ω_- . Thus, along each level set of x_3 , $|x_3^*(p)| \rightarrow \infty$ and so z is onto. Then, by the level set analysis in the proof of 3.4.1 and Picard's theorem, $f \circ z^{-1}$ is a polynomial and is indeed linear. \square

3.4.2 Concluding Uniqueness

After a translation in \mathbb{R}^3 and a rebasing of x_3^* , $f(z) = \alpha z$ for some $\alpha \in \mathbb{C}$. As dz is the height differential, the Weierstrass representation gives

$$x_1(it) = |\alpha|^{-2} (\alpha_2 \sinh(\alpha_2 t) \sin(\alpha_1 t) - \alpha_1 \cosh(\alpha_2 t) \cos(\alpha_1 t))$$

and

$$x_2(it) = |\alpha|^{-2} (\alpha_2 \sinh(\alpha_2 t) \cos(\alpha_1 t) + \alpha_1 \cosh(\alpha_2 t) \sin(\alpha_1 t))$$

where $\alpha = \alpha_1 + i\alpha_2$. By inspection this curve is only embedded when $\alpha_1 = 0$, i.e. if $\alpha = i\alpha_2$. The factor α_2 corresponds to a homothetic rescaling and so Σ is the helicoid.

Chapter 4

Conformal Structure of Minimal Surfaces with Finite Topology

Throughout this section, we apply the techniques of Chapter 3 to study complete embedded minimal surfaces with finite topology and one end. The space $\mathcal{E}(1)$ of such surfaces is non-trivial; the embedded genus one helicoid, \mathcal{H} , constructed in [22] by Hoffman, Weber, and Wolf provides an example which moreover has the property of being asymptotically helicoidal (see also [32] for a good exposition). We note again that Colding and Minicozzi, in [13], show that any surface in $\mathcal{E}(1)$ is necessarily properly embedded, a fact we use throughout.

The construction and study of \mathcal{H} , as well as objects in the larger class where embeddedness is dropped, has a rich history. Using the Weierstrass representation, Hoffman, Karcher, and Wei in [20] first constructed an immersed genus one helicoid. Computer graphics suggested it was embedded, but the existence of an embedded

genus one helicoid (in fact \mathcal{H}) followed only after Hoffman and Wei proposed a new construction in [23]. They considered \mathcal{H} as the limit of a family of screw-motion invariant minimal surfaces with periodic handles and a helicoidal end. Weber, Hoffman, and Wolf confirmed the existence of such a family of surfaces in [21] and ultimately proved embeddedness of \mathcal{H} in [22]. Hoffman, Weber, and Wolf conjecture that \mathcal{H} is the unique element of $\mathcal{E}(1)$ with genus one containing two coordinate axes. Recently, Hoffman and White, in [25], used a variational argument to construct an embedded genus one helicoid, though whether their construction is \mathcal{H} is unknown.

In [24], Hoffman and White proved rigidity results for immersed minimal genus one surfaces with one end, assuming the surface contained the x_1 and x_3 -axes. In particular, they showed the surface was conformally a punctured torus with the end asymptotic to a helicoid. In this section, we prove Theorem 1.1.4. That is, we show that any $\Sigma \in \mathcal{E}(1)$ is conformally a once punctured, compact Riemann surface, with Weierstrass data that has helicoid-like behavior at the puncture.

As in the simply connected case, the proof of Theorem 1.1.4 requires we first prove the strong structural decomposition result, Theorem 1.2.1.

4.1 Decomposition of Σ

In the next four subsections, we develop the tools needed to prove the structural results of Theorem 1.2.1 and Proposition 1.2.3. Many of these are extensions of those developed for the simply connected case. We prove Theorem 1.2.1 and Proposition 1.2.3 at the conclusion of subsection 4.1.9.

4.1.1 Preliminaries

We first introduce some notation. Throughout this chapter, let $\Sigma \in \mathcal{E}(1)$ and have positive genus, i.e. Σ is a complete, properly embedded minimal surface with finite and positive genus, k , and one end. Here we say that a surface has genus k if it is homeomorphic to a compact genus k Riemann surface with at most a finite number of punctures. As Σ has one end and is complete in \mathbb{R}^3 , there exists an $R > 0$ so that one of the components $\overline{\Sigma}$ of $\Sigma \cap B_R$ is a compact surface with connected boundary and genus k . Thus, $\Sigma \setminus \overline{\Sigma}$ has genus 0 and is a neighborhood of the end of Σ . We now homothetically rescale so that the genus, $\overline{\Sigma}$, lies in B_1 and so that $\sup_{\overline{\Sigma}} |A|^2 \geq 1$.

We continue to let $\mathbf{C}_\delta = \{x_3^2 \leq \delta^2(x_1^2 + x_2^2)\}$, as in Definition 3.1.1. Further, we still refer to a blow-up pair (y, s) as in Definition 3.1.4.

4.1.2 Topological structure of Σ

An elementary but crucial consequence of the maximum principle is that each component of the intersection of a minimal disk with a closed ball is a disk. Similarly, each component of the intersection of a genus k surface with a ball has genus at most k (see Appendix C of [12] and Section I of [11]). We note that for Σ with one end and finite genus we obtain a bit more:

Proposition 4.1.1. *Suppose $\Sigma \in \mathcal{E}(1)$ and $\overline{\Sigma} \subset \Sigma \cap B_1$ is connected and has the same genus as Σ . Then, $\Sigma \setminus \overline{\Sigma}$ is an annulus. Moreover, for any convex set C with non-empty interior, if $C \cap B_1 = \emptyset$, then each component of $C \cap \Sigma$ is a disk. Alternatively, if $B_1 \subset C$ then all the components of $C \cap \Sigma$ not containing $\overline{\Sigma}$ are disks.*

Proof. That $\Sigma \setminus \bar{\Sigma}$ is an annulus is a purely topological consequence of Σ having one end. Namely, if $\partial\bar{\Sigma}$ had more than one connected component, the genus of Σ would be strictly greater than the genus of $\bar{\Sigma}$.

If C and B_1 are disjoint then, as they are convex, there exists a plane P so that P meets Σ transversely and so that P separates B_1 and C . Since $\Sigma \setminus \bar{\Sigma}$ is an annulus and $P \cap \bar{\Sigma} = \emptyset$, the convex hull property implies that $P \cap \Sigma$ consists only of unbounded smooth proper curves. Thus exactly one of the components of $\Sigma \setminus (P \cap \Sigma)$ is not a disk. As C is disjoint from the non-disk component we have the desired result. On the other hand, if C is convex and contains B_1 , denote by C' the component of $C \cap \Sigma$ containing $\bar{\Sigma}$. Suppose there was a component of $C \cap \Sigma$ not equal to C' that was not a disk, then there would be a subset of Σ with boundary in \bar{C} but interior disjoint from C , violating the convex hull property. \square

4.1.3 Rescalings of Σ

We note that Theorem 1.2.1 is a sharpening, for $\Sigma \in \mathcal{E}(1)$, of a much more general description of the shapes of minimal surfaces given by Colding and Minicozzi in [4]. More precisely, in that paper they show, for a large class of embedded minimal surfaces in \mathbb{R}^3 , how the geometric structure of a surface is determined by its topological properties. In particular, as Σ has finite topology and one end, their work shows that it roughly looks like a helicoid. That is, away from a compact set containing the genus, Σ is made up of two infinite-valued graphs that spiral together and are glued along an axis. While we do not make direct use of this description, it is needed in

order to derive the structural results of Section 4.1.4 from the compactness theory of [4]. Thus, we briefly sketch a proof.

First, Theorem 4.1.1 implies that the sequences $\lambda_i \Sigma$, $\lambda_i \rightarrow 0$, of homothetic scalings of Σ are all uniformly locally simply connected (ULSC); i.e. there is no concentration of topology other than the genus shrinking to a point (see (1.1) of [4] for the rigorous definition). Theorem 0.9 of [4] (particularly its extension to finite genus ULSC surfaces) gives a compactness result for such sequences. Namely, any ULSC sequence of fixed, finite genus surfaces, with boundaries going to ∞ and curvature blowing up in a compact set, has a subsequence converging to a foliation, \mathcal{L} , of flat parallel planes with at most two singular lines (where the curvature blows up), $\mathcal{S}_1, \mathcal{S}_2$ orthogonal to the leaves of the foliation. Up to a rotation of \mathbb{R}^3 we have $\mathcal{L} = \{x_3 = t\}_{t \in \mathbb{R}}$ and so \mathcal{S}_i are parallel to the x_3 -axis. Away from the singular lines the convergence is in the sense of graphs, in the C^α topology on compact sets for any $0 < \alpha < 1$. Moreover, as explained in property (C_{ulsc}) of Theorem 0.9 (see also Proposition 1.5 of [4]), in a small ball centered at a point of the singular set the convergence is (away from the singular set) as a double spiral staircase. We note that in our case, i.e. $\lambda_i \Sigma, \lambda_i \rightarrow 0$, there is only one singular line and indeed since $\overline{\Sigma} \subset B_1$ has non-zero curvature this singular line is the x_3 -axis. To see this, we use a further description of the convergence given by property (C_{ulsc}) , namely, when there are two singular lines, the double spirals that form around each singular line are glued so that graphs going around both singular lines close up. To be precise, consider bounded, non-simply connected subsets of $\mathbb{R}^3 \setminus (\mathcal{S}_1 \cup \mathcal{S}_2)$ that contain no closed curves homo-

topic (in $\mathbb{R}^3 \setminus (\mathcal{S}_1 \cup \mathcal{S}_2)$) to a curve around only \mathcal{S}_i . That is, consider bounded regions that go only around both singular lines. In these regions, the convergence is as a single valued graph. If this were true of the convergence of $\lambda_i \Sigma$, then one could remove from Σ a closed curve disjoint from $\overline{\Sigma}$ and obtain two unbounded components, contradicting that Σ has one end. Thus, the local picture near \mathcal{S}_1 of a double spiral staircase extends outward and Σ has the claimed structure.

4.1.4 Structural Results

To obtain the decomposition of Theorem 1.2.1 we will need two important structural results which generalize results for disks from [9] and [10] (it should be noted that many of the proofs of these results did not require that the surface be a disk but only that the boundary be connected, a fact used in [4]). The first is the existence of an N -valued graph starting near the genus and extending as a graph all the way out. The second result is similar but for a blow-up pair far from the genus. Namely, for such a pair, a multivalued graph forms on the scale of the pair and extends as a graph all the way out. It may be helpful to compare with the comparable results for disks, i.e. Theorem 0.3 of [9] and Theorem 0.4 of [10].

The geometric nature of the proof of Theorem 0.9 of [4] implies that $\lambda_i \Sigma$ always converges to the same lamination independent of the choice of λ_i . We now use the nature of this convergence, that any sequence of homothetic rescalings $\lambda_i \Sigma$, with $\lambda_i \rightarrow 0$, has a subsequence that converges to the foliation \mathcal{L} with singular set \mathcal{S} , the x_3 -axis, to deduce gradient bounds in a cone. This, and further application of the

compactness theory, will then give Propositions 4.1.3 and 4.1.4.

Lemma 4.1.2. *For any $\epsilon > 0, \delta > 0$ there exists an $R > 1$ so every component of $(\mathbf{C}_\delta \setminus B_R) \cap \Sigma$ is a graph over $\{x_3 = 0\}$ with gradient less than ϵ .*

Proof. We proceed by contradiction. Suppose there exists a sequence $\{R_i\}$ with $R_i \rightarrow \infty$ and points $p_i \in (\mathbf{C}_\delta \setminus B_{R_i}) \cap \Sigma$ such that the component of $B_{\gamma|p_i|}(p_i) \cap \Sigma$ containing p_i , Ω_i , is not a graph over $\{x_3 = 0\}$ with gradient less than ϵ . Here γ depends on δ and will be specified later. Now, consider the sequence of rescalings $\frac{1}{|p_i|}\Sigma$, which by possibly passing to a subsequence converges to \mathcal{L} . Passing to another subsequence, $\frac{1}{|p_i|}p_i$ converges to a point $p_\infty \in \mathbf{C}_\delta \cap B_1$. Let $\tilde{\Omega}_i = \frac{1}{|p_i|}\Omega_i$. Proposition 1.5 of [4] guarantees that if $B_\gamma(p_\infty) \cap \mathcal{S} = \emptyset$ then the $\tilde{\Omega}_i$ converge to $\tilde{\Omega}_\infty \subset \{x_3 = x_3(p_\infty)\}$ as graphs. As \mathcal{S} is the sole singular set, we may choose γ sufficiently small, depending only on δ , to make this happen. Thus, for sufficiently large j , $\tilde{\Omega}_j$ is a graph over $\{x_3 = 0\}$ with gradient bounded by ϵ , giving the desired contradiction. \square

Note that variants of the following propositions are used in [4], specifically in the proof of the compactness result, i.e. Theorem 0.9 for finite genus surfaces, though they are not made explicit there. Note that while both propositions require a rotation of \mathbb{R}^3 , they are the same rotation. This can be seen because we prove both propositions by a compactness argument that appeals to the Colding-Minicozzi lamination theory of [4]. The only rotation needed is the initial rotation required in Theorem 0.9 of [4].

Proposition 4.1.3. *Given $\epsilon > 0$ and $N \in \mathbb{Z}^+$ there exists an $R > 0$ so that: After a rotation of \mathbb{R}^3 there exists an N -valued graph $\Sigma_g \subset \Sigma$ over the annulus $D_\infty \setminus D_R \subset \{x_3 = 0\}$, with gradient bounded by ϵ and in \mathbf{C}_ϵ .*

Proof. Choose R from Lemma 4.1.2 with $\delta = \epsilon$. Note, control on the gradient bounds the separation between sheets. Thus, increasing R , if necessary, guarantees N sheets of a graph inside \mathbf{C}_ϵ . \square

Proposition 4.1.4. *Given $\epsilon > 0$ sufficiently small and $N \in \mathbb{Z}^+$ there exist $C_1, C_2 > 0$ and $R > 0$ so: After a rotation of \mathbb{R}^3 , if (y, s) is a C_1 blow-up pair in Σ and $|y| \geq R$ then there exists an N -valued graph Σ_g over the annulus $D_\infty \setminus D_s(\Pi(y)) \subset \{x_3 = 0\}$ with gradient bounded by ϵ and in the cone $\mathbf{C}_\epsilon(y)$, with initial separation bounded below by C_2s . Finally, $\text{dist}_\Sigma(\Sigma_g, y) \leq 2s$.*

Proof. Note that as long as $|y|$ is sufficiently large, Theorem 0.6 of [10] gives an $\Omega < 1/2$ (as well as C_1 and C_2) so that since the component of $B_{\frac{1}{2}|y|}(y) \cap \Sigma$ containing y is a disk, there exists a N -valued graph Σ_0 over the annulus, $A = D_{\Omega|y|} \setminus D_{s/2}(y) \subset P$ with gradient bounded by $\epsilon/2$, initial separation greater than C_2s and $\text{dist}_\Sigma(\Sigma_0, y) \leq 2s$. Here P is in principle an arbitrary plane in \mathbb{R}^3 .

We claim that Lemma 4.1.2 implies a subset, Σ'_0 , of Σ_0 is a N -valued graph over the annulus $A' = D_{\Omega|y|/2} \setminus D_s(\Pi(y)) \subset \{x_3 = 0\}$ with gradient bounded by ϵ , which further implies Σ'_0 can be extended as desired. To that end we note that for $\delta > 1/(4\Omega)$, if $y \notin \mathbf{C}_\delta$ then A (and thus, by possibly increasing δ , Σ_0) meets \mathbf{C}_δ . Lemma 4.1.2 allows us to choose an $R_0 > 0$ so that every component of $\Sigma \cap (\mathbf{C}_\delta \setminus B_{R_0})$ is a multi-valued graph over $\{x_3 = 0\}$ with gradient bounded by $\epsilon/4$. Thus if we take $R > 2R_0$ then there is a point of Σ_0 in $\mathbf{C}_\delta \setminus B_{R_0}$; therefore, for the gradient estimates at the point to be consistent, P must be close enough to $\{x_3 = 0\}$ so that we may choose $\Sigma'_0 \subset \Sigma_0$ so it is a multi-valued graph over A' . Furthermore, the part of Σ'_0

over the outer boundary of A' is necessarily inside of $\mathbf{C}_\delta \setminus B_{R_0}$ and so Lemma 4.1.2 allows us to extend it as desired. \square

4.1.5 One-sided Curvature in Σ

In several places we make use of the one-sided curvature estimate of [12]. Recall that this result gives a curvature estimate for a minimal disk that is close to and on one side of a plane. As a sequence of rescaled catenoids shows, it is crucial that the surface be a disk. In our situation, Proposition 4.1.1 allows the use of the one-sided curvature estimate far from the genus. For convenience we record the statement we will need and indicate how it follows from 2.4.2

Corollary 4.1.5. *Given $\epsilon, \delta > 0$ there exist $\delta_0 > 0$ and $R > 1$ such that, if there exists a 2-valued δ_0 -sheet on scale s centered at y where $y \notin \mathbf{C}_\delta \cup B_R$, then all the components of $\Sigma \cap (\mathbf{C}_{\delta_0} \setminus B_{2s}(y))$ are multi-valued graphs with gradient $\leq \epsilon$.*

Proof. The result follows immediately from the proof of Corollary 2.4.2 of [12] as long as one notes that the proof of I.1.9 depends only on each component of $\Sigma \cap \mathbf{C}_{K\delta_0}$ being a disk for K some large (universal) constant. Thus, by Proposition 4.1.1, we need only check that for a suitable choice of R and upper bound δ'_0 for δ_0 (both R and δ'_0 depending only on δ), $y \notin \mathbf{C}_\delta \cup B_R$ implies $\mathbf{C}_{K\delta'_0}(y)$ is disjoint from B_1 (i.e. from the genus).

Now suppose $x \in \mathbf{C}_{K\delta'_0}(y)$ and think of x and y as vectors. By choosing δ'_0 sufficiently small (depending on δ) we have that $|\langle x - y, y \rangle| < (1 - \gamma)|y||x - y|$ (that is the angle between $x - y$ and y is bounded away from 0°); note $1 > \gamma > 0$ depends

only on δ . But then $|x|^2 = |x - y + y|^2 \geq |x - y|^2 + 2\langle x - y, y \rangle + |y|^2 \geq \gamma|y|^2$. Hence, picking $R^2 > \frac{1}{\gamma}$ suffices. \square

4.1.6 Geometric Bounds Near Blow-up Pairs

We record the following extension of Lemma 2.26 of [13] to surfaces with non-trivial topology. The proof is identical to that of Lemma 2.26 as long as one replaces Colding and Minicozzi's compactness result for minimal disks, i.e. Theorem 0.1 of [12], with the more general Theorem 0.6 of [4]:

Proposition 4.1.6. *Given K_1, g we get a constant K_2 such that if*

1. $\Sigma \subset \mathbb{R}^3$ is an embedded minimal surface with $\text{genus}(\Sigma) = g$
2. $\Sigma \subset B_{K_2 s}(y)$ and $\partial\Sigma \subset \partial B_{K_2 s}(y)$
3. (y, s) is a blow-up pair,

then we get the curvature bound

$$(4.1) \quad \sup_{B_{K_1 s}(y) \cap \Sigma} |A|^2 \leq K_2 s^{-2}.$$

An immediate corollary is that, for blow-up pairs far from the genus, the scale is small relative to distance to the genus.

Corollary 4.1.7. *Given $\alpha, C_1 > 0$ there exists an R such that for (y, s) , a C_1 blow-up pair of Σ with $|y| \geq R$ then $s < \alpha|y|$.*

Proof. Recall we have normalized Σ so $\sup_{B_1 \cap \Sigma} |A|^2 \geq 1$. Now suppose the result did not hold. Then there exists a sequence (y_j, s_j) of C_1 blow-up pairs with $|y_j| \geq j$ and $s_j \geq \alpha|y_j|$. Set $K_1 = 2/\alpha$. By Proposition 4.1.6 there exists K_2 such that $\sup_{B_{K_1 s_j}(y_j) \cap \Sigma} |A|^2 \leq K_2 s_j^{-2}$. Since $B_1 \subset B_{K_1 s_j}(y_j)$, $\sup_{B_1 \cap \Sigma} |A|^2 \leq K_2 s_j^{-2}$. But $s_j \geq \alpha|y_j| \geq \alpha j$, thus for j sufficiently large one obtains a contradiction. \square

4.1.7 Blow-up Sheets

In order to get the strict spiraling in the decomposition of Theorem 1.2.1 we need to check that the multi-valued graphs that make up most of Σ can be consistently normalized. To that end, we note that for blow-up pairs far enough from the genus one obtains a nearby ϵ -sheet (i.e. we have a normalized multivalued graph). Indeed, the proof of Theorem 3.1.5 of Chapter 3 applies without change to blow-up pairs satisfying the conditions of Proposition 4.1.4. We claim that in between this sheet, Σ consists of exactly one other ϵ -sheet.

Theorem 4.1.8. *Given $\epsilon > 0$ sufficiently small there exist $C_1, C_2 > 0$ and $R > 1$ so: Suppose (y, s) is a C_1 blow-up pair, with $|y| > R$. Then there exist two 4-valued ϵ -sheets $\Sigma_i = \Gamma_{u_i}$ ($i = 1, 2$) on the scale s centered at y which spiral together (i.e. $u_1(s, 0) < u_2(s, 0) < u_1(s, 2\pi)$). Moreover, the separation over $\partial D_s(\Pi(y))$ of Σ_i is bounded below by $C_2 s$.*

Remark 4.1.9. We refer to Σ_1, Σ_2 as (ϵ) -blow-up sheets associated with (y, s) .

Proof. We fix a $\delta > 0$ and note that Lemma 4.1.2 gives a $R > 1$ so that if $|y| > R$ then $y \notin \mathbf{C}_\delta$ and using this δ and ϵ we pick $\delta_0 < \epsilon$ as in Corollary 4.1.5 (and increase

R if needed). Then, Theorem 3.1.5 of Chapter 3 and Proposition 4.1.4 together give one δ_0 -sheet, Σ_1 , forming near (y, s) for appropriately chosen C_1 (and possibly after again increasing R). Now as long as the part of Σ between the sheets of Σ_1 make up a second minimal graph, the proof of Theorem 3.1.8 of Chapter 3 applies (and provides the correct C_2).

We denote by E the region in \mathbb{R}^3 between the sheets of Σ_1 (see Theorem I.0.10 of [12] or Theorem 3.1.8 of Chapter 3 for a precise definition). Theorem I.0.10 of [12] implies that near the blow-up pair the part of Σ between Σ_1 is a graph Σ_2^{in} ; i.e. if R_0 is chosen so $B_{4R_0}(y)$ is disjoint from the genus then $B_{R_0}(y) \cap E \cap \Sigma \setminus \Sigma_1 = \Sigma_2^{in}$. To ensure Σ_2^{in} is non-empty, we increase R so that $|y| \geq 8s$ (which we may do by Corollary 4.1.7). On the other hand, Appendix D of that same paper guarantees that, outside of a very large ball centered at the genus, the part of Σ between Σ_1 is a graph, Σ_2^{out} . That is, for $R_1 \geq |y|$ large, $E \cap \Sigma \setminus (B_{R_1} \cup \Sigma_1) = \Sigma_2^{out}$. Now by one-sided curvature estimates (which Corollary 4.1.5 allows us to use), all the components of $E \setminus \Sigma_1$ are graphs and so it suffices to show that Σ_2^{in} and Σ_2^{out} are subsets of the same component. Suppose not. Then, as Σ_2^{in} is a graph and Σ is complete, Σ_2^{in} must extend inside E beyond B_{R_1} . But this contradicts Appendix D of [12] by giving two components of $\Sigma \setminus \Sigma_1$ in $E \cap \Sigma \setminus B_{R_1}$. \square

4.1.8 Blow-Up Pairs

While the properties of ϵ -sheets give the strictly spiraling region of Σ , to understand the region where these sheets fit together (i.e. the axis), we need a handle on the

distribution of the blow-up pairs of Σ . In the case of trivial topology, non-flatness gives one blow-up pair (y_0, s_0) , which in turn yields associated blow-up sheets. Then by Corollary III.3.5 of [11], the blow-up sheets give the existence of nearby blow-up pairs $(y_{\pm 1}, s_{\pm 1})$ above and below (see also Theorem 3.1.10 of Chapter 3 or Lemma 2.5 of [13]). Iterating, one constructs a sequence of blow-up pairs that give the axis \mathcal{R}_A .

Crucially, for the extension of the argument to surfaces in $\mathcal{E}(1)$, the result of [11] is local; it depends only on the topology being trivial in a large ball relative to the scale s_0 . Thus, the above construction holds in Σ as long as one deals with two issues. First, establish the existence of two initial blow-up pairs far from the genus, one above and the other below, with small scale relative to the distance to the genus. Second, show that the iterative process produces blow-up pairs which continue to have small scale (again relative to the distance to the genus).

We claim that the further a blow-up pair is from the genus, the smaller the ratio between the scale and the distance to the genus; hence both issues can be addressed simultaneously. This is an immediate consequence (see Corollary 4.1.7) of the control on curvature around blow-up pairs as given by Proposition 4.1.6 (an extension of Lemma 2.26 of [13] to Σ). Thus, given an initial blow-up pair far enough above the genus, we can iteratively produce higher and higher blow-up pairs that satisfy the appropriate scale condition, with the same true starting below the genus and going down. Here we establish the existence of a chain of blow-up pairs which will be critical to our decomposition theorem:

Lemma 4.1.10. *Given $\epsilon > 0$ sufficiently small, there exist constants $C_1, C_{in} > 0$ and*

a sequence $(\tilde{y}_i, \tilde{s}_i)$ of C_1 blow-up pairs of Σ such that: the sheets associated to $(\tilde{y}_i, \tilde{s}_i)$ are ϵ -sheets on scale \tilde{s}_i centered at \tilde{y}_i and $x_3(\tilde{y}_i) < x_3(\tilde{y}_{i+1})$ for $i \geq 1$, $\tilde{y}_{i+1} \in B_{C_{in}\tilde{s}_i}(\tilde{y}_i)$ while for $i \leq -1$, $\tilde{y}_{i-1} \in B_{C_{in}\tilde{s}_i}(\tilde{y}_i)$.

Proof. Without loss of generality, we work above the genus (i.e. for $x_3 > 1$ and $i \geq 1$), as the argument below the genus is identical. Use ϵ to choose C_1, C_2 and R as in Theorem 3.1.8. By Corollary III.3.5 of [11] there are constants $C_{out} > C_{in} > 0$ such that, for a C_1 blow-up pair (y, s) with $|y| \geq R$, as long as the component of $B_{C_{out}s}(y) \cap \Sigma$ containing y is a disk, we can find blow-up pairs above and below (y, s) and inside $B_{C_{in}s}(y)$. Corollary 4.1.7 and Proposition 4.1.1 ensure a value $h_1 \geq R$, depending on C_{out} so for $|y| \geq h_1$ this condition is satisfied. Thus, it suffices to find an initial blow-up pair $(\tilde{y}_1, \tilde{s}_1)$ with $|\tilde{y}_1| \geq h_1$, as repeated application of Corollary III.3.5 of [11] will give the sequence $(\tilde{y}_i, \tilde{s}_i)$.

Proposition 4.1.3 and Appendix D of [12] together guarantee the existence of two \tilde{N} -valued graphs spiraling together over an unbounded annulus (with inner radius \bar{R}). Then, for large enough \tilde{N} , the proof of Theorem 3.1.8 of Chapter 3 gives two N -valued ϵ -sheets around the genus, Σ_1, Σ_2 , on some scale \tilde{R} and in the cone \mathbf{C}_ϵ . Theorem III.3.1 of [11] with $r_0 \geq \max\{1, \tilde{R}, h_1\}$ then implies there is large curvature above and below the genus. Hence, by a standard blow-up argument (see Lemma 5.1 of [10]) one gets the desired C_1 blow-up pair $(\tilde{y}_1, \tilde{s}_1)$ above the genus with $|\tilde{y}_1| > 2r_0 \geq h_1$. \square

4.1.9 Decomposing Σ

In this section, we provide proofs of Proposition 1.2.3 and Theorem 1.2.1. They follow immediately after the proof of the structural decomposition.

The decomposition of Σ now proceeds as in Section 3.2 of Chapter 3, with Proposition 3.2.3 of Chapter 3 giving strict spiraling far enough out in the ϵ -sheets of Σ . After specifying the region of strict spiraling, \mathcal{R}_S , the remainder of Σ will be split into the genus, \mathcal{R}_G , and the axis, \mathcal{R}_A . The strict spiraling, the fact that away from the genus convex sets meet Σ in disks (see Lemma 4.1.1), and the proof of Rado's theorem (see [30]) will then give $\nabla_{\Sigma}x_3 \neq 0$ in \mathcal{R}_A . A Harnack inequality will then allow us to obtain a lower bound for $|\nabla_{\Sigma}x_3|$ on this set.

Lemma 4.1.11. *There exist constants C_1, R_0, R_1 and a sequence (y_i, s_i) ($i \neq 0$) of C_1 blow-up pairs of Σ so that: $x_3(y_i) < x_3(y_{i+1})$ and for $i \geq 1$, $y_{i+1} \in B_{R_1 s_i}(y_i)$ while for $i \leq -1$, $y_{i-1} \in B_{R_1 s_i}(y_i)$. Moreover, if $\mathcal{R}_A = \mathcal{R}_A^+ \cup \mathcal{R}_A^-$ where \mathcal{R}_A^{\pm} is $\bigcup_{\pm i > 0} \Sigma_{R_1 s_i, y_i}$ (and $\Sigma_{R_1 s_i, y_i}$ is the component of $B_{R_1 s_i}(y_i) \cap \Sigma$ containing y_i), then $\mathcal{R}_S = \Sigma \setminus (\mathcal{R}_A \cup B_{R_0})$ has exactly two unbounded components which can be written as the union of two multi-valued graphs u^1 and u^2 , with $u_{\theta}^i \neq 0$.*

Proof. We wish to argue as in Lemma 3.3.1 of Chapter 3 and to do so we must ensure that we may use the chord-arc bounds of [13] and the one-sided curvature estimates of [12] near the pairs (y_i, s_i) . As these are both local results it will suffice to work far from the genus.

Fix $\epsilon < \epsilon_0$ where ϵ_0 is given by Proposition 3.2.3 of Chapter 3 which will be important for the strict spiraling. Next pick $\delta > 0$ and apply Corollary 4.1.5 to

obtain a $\delta_0 < \epsilon$ and $\tilde{R} > 1$. Now using δ_0 in place of ϵ let $(\tilde{y}_i, \tilde{s}_i)$ be the sequence constructed in Lemma 4.1.10. Let us now determine how to choose the (y_i, s_i) .

First of all, as long as $y_i \notin \mathbf{C}_\delta \cup B_{\tilde{R}}$ we may use the one-sided curvature estimate in $\mathbf{C}_{\delta_0}(y_i)$. Notice by Lemma 4.1.2 we may increase \tilde{R} and require only that $y_i \notin B_{\tilde{R}}$. Now recall that the chord-arc bounds give a constant $C_{arc} > 0$ so for any $\gamma > 1$, if the component of $B_{2C_{arc}\gamma s_i}(y_i) \cap \Sigma$ containing y_i is a disk, then the intrinsic ball of radius $C_{arc}\gamma s_i$ centered at y_i contains $B_{\gamma s_i}(y_i) \cap \Sigma$. On (y_i, s_i) , we want a uniform bound, N , on the number of sheets between the blow-up sheets associated to the pairs (y_i, s_i) and (y_{i+1}, s_{i+1}) . This is equivalent to a uniform area bound which in turn follows from the chord-arc bounds described above and curvature bounds of Proposition 4.1.6 (for details see Proposition 3.1.11 of Chapter 3). To correctly apply this argument, one must be sufficiently far from the genus; i.e. for a fixed constant C_{bnd} , the component of $B_{C_{bnd}s_i}(y_i) \cap \Sigma$ containing y_i must be a disk. To that end, pick $h_2 \geq 0$ by using Corollary 4.1.7 with $\alpha^{-1} \geq \max\{C_{bnd}, 2R_1, \tilde{R}\}$ where R_1 is to be chosen later. We then pick the sequence (y_i, s_i) from $(\tilde{y}_i, \tilde{s}_i)$ by requiring $x_3(y_i) \geq h_2$ (and then relabelling). Notice that the way we choose the (y_i, s_i) ensures that N is independent of our ultimate choice of R_1 .

We now determine R_1 . By choice of (y_i, s_i) , the one-sided curvature bounds hold and so there is an R_2 such that in $\mathbf{C}_{\delta_0}(y_1)$ all of the (at most) N sheets between the blow-up sheets associated to (y_1, s_1) and (y_2, s_2) are δ_0 -sheets on scale $R_2 s_1$ centered on the line ℓ which goes through y_1 and is parallel to the x_3 -axis (see Theorem 3.1.6 of Chapter 3). Label these pairs of δ_0 -sheets Σ_k^j , $k = 1, 2$ and $1 \leq j \leq N$. Proceeding

now as in the second paragraph of the proof of Lemma 3.3.1 in Chapter 3, we use N , C_2 and (2.5) to get \tilde{C}_2 so $\tilde{C}_2 s_1$ is a lower bound on the separation of each Σ_k^j over the circle $\partial D_{R_2 s_1}(\Pi(y_1)) \subset \{x_3 = 0\}$. Proposition 3.2.3 of Chapter 3 gives a C_3 , depending on \tilde{C}_2 , such that outside of a cylinder centered at ℓ of radius $R_2 C_3 s_1$, all the Σ_k^j strictly spiral. Choose \tilde{R}_1 , depending only on C_{in} , N , δ_0 , C_3 and R_2 , so $B_{\tilde{R}_1 s_1}(y_1)$ contains this cylinder, the point y_2 and meets each Σ_k^j . Then if $R_1 = C_{arc} \tilde{R}_1$ the preceding is also true of the component of $B_{R_1 s_1}(y_1) \cap \Sigma$ containing y_1 . By the scaling invariance of strict spiraling and the uniformity of the choices, the same is true for each (y_i, s_i) .

Finally, by properness, there exists a finite number, M , of ϵ -sheets between the blow-up sheets associated to $(y_{\pm 1}, s_{\pm 1})$. Pick R_0 large enough so that outside of the ball of radius R_0 the M sheets between the blow-up sheets associated to (y_1, s_1) and (y_{-1}, s_{-1}) strictly spiral. Such an R_0 exists by Proposition 4.1.3 and the above argument. \square

Proof. (Proposition 1.2.3) By properness there exists an $R'_0 \geq R_0$ so that the component of $B_{R'_0} \cap \Sigma$ containing $\bar{\Sigma}$ contains $B_{R_0} \cap \Sigma$. We take \mathcal{R}_G to be this component and note that $\partial \mathcal{R}_G$ is connected by Proposition 4.1.1. The strict spiraling in \mathcal{R}_S and the proof of Rado's theorem gives Proposition 1.2.3. \square

Proof. (Theorem 1.2.1) By using Lemma 4.1.11 (and making the obvious modifications needed to account for \mathcal{R}_G) the proof of Theorem 3.0.3 of Chapter 3 then gives Theorem 1.2.1 of this paper. \square

4.2 Conformal Structure of Γ

In this section we prove Theorem 1.1.4 and Corollary 1.1.6 (in subsection 4.2.3) by analysis similar to that in Section 3.4 of Chapter 3. To do so, we first show that $\Gamma = \Sigma \setminus \mathcal{R}_G$ is conformally a punctured disk and, indeed, the map $z = x_3 + ix_3^* : \Gamma \rightarrow \mathbb{C}$ is a proper, holomorphic coordinate (here x_3^* is the harmonic conjugate of x_3). Note that by Proposition 1.2.3, as long as z is well defined, it is injective and a conformal diffeomorphism. Thus, it suffices to check that z is well defined and that it is proper; i.e. if $p \rightarrow \infty$ in Γ then $z(p) \rightarrow \infty$.

Proposition 4.2.1. *x_3^* is well defined on Γ .*

Proof. As Σ is minimal, $*dx_3$, the conjugate differential to dx_3 , exists on Σ and is closed and harmonic. We wish to show it is exact on Γ . To do so, it suffices to show that for every closed curve ν in Γ , we have $\int_\nu *dx_3 = 0$. By Proposition 4.1.1, $\Sigma \setminus \nu$ has two components, only one of which is bounded. The bounded component, together with ν , is a manifold with (connected) boundary, and on this manifold $*dx_3$ is a closed form. Hence, the result follows immediately from Stokes' theorem. \square

4.2.1 Existence of f

We now show that there exists $f : \Gamma \rightarrow \mathbb{C}$ such that $g = e^f$ on Γ , where g is the stereographic projection of the Gauss map of Σ . We argue as in Section 3.4 of Chapter 3, though we must first check that there is a well defined notion of $\log g$ in Γ . Since g is meromorphic in Σ and has no poles or zeros in Γ , this is equivalent to showing that g has an equal number of poles and zeros.

Proposition 4.2.2. *Counting multiplicity, g has an equal number of poles and zeros.*

Proof. The zeros and poles of g occur only at the critical points of x_3 . In particular, by Proposition 3.0.5, there exist h and R so that all the zeros and poles are found in the cylinder:

$$(4.2) \quad C_{h,R} = \{|x_3| \leq h, x_1^2 + x_2^2 \leq R^2\} \cap \Sigma.$$

Moreover, for R and h sufficiently large, $\gamma = \partial C_{h,R}$ is the union of four smooth curves, two at the top and bottom, γ_t and γ_b , and two disjoint helix like curves $\gamma_1, \gamma_2 \subset \mathcal{R}_S$. Hence, for $c \in (-h, h)$, $\{x_3 = c\}$ meets $\partial C_{h,R}$ in exactly two points. Additionally, as γ_1 and γ_2 are compact, there is a constant $\alpha > 0$ so $|\frac{d}{dt}x_3(\gamma_i(t))| > \alpha$, $i = 1, 2$.

Let us first suppose that g has only simple zeros and poles and these occur at distinct values of x_3 , thus, the Weierstrass representation implies that the critical points of x_3 are non-degenerate. We now investigate the level sets $\{x_3 = c\}$. By the strict spiraling of γ_i ($i = 1, 2$), at the regular values these level sets consist of an interval with end points in γ_i ($i = 1, 2$) and the union of a finite number of closed curves. Moreover, by the minimality of $C_{h,R}$, the non-smooth components of the level sets at critical values will consist of either two closed curves meeting in a single point or the interval and a closed curve meeting in a single point. As a consequence of this $\{|x_3| \leq h, x_1^2 + x_2^2 \leq R^2\} \setminus C_{h,R}$ has exactly two connected components Ω_1 and Ω_2 . Orient $C_{h,R}$ by demanding that the normal point into Ω_1 . Notice that it is well defined to say if a closed curve appearing in $\{x_3 = c\} \cap C_{h,R}$ surrounds Ω_1 or Ω_2 .

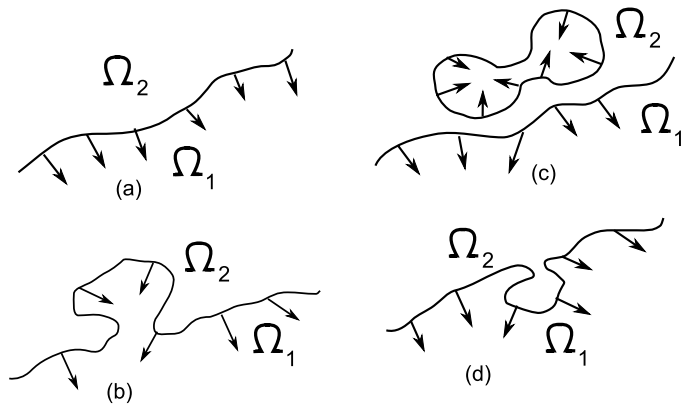


Figure 4.1: Level curve examples in Proposition 4.2.2

The restrictions imposed on g and minimality of $C_{h,R}$ imply that at any critical level, as one goes downward, either a single closed curve is “created” or is “destroyed”. (See Figure 4.1*.) Moreover, when such a curve is created it makes sense to say whether it surrounds Ω_1 or Ω_2 and this is preserved as one goes downward. Now suppose a closed curve is created and that it surrounds Ω_1 ; then it is not hard to see that at the critical point the normal must point upwards. Similarly, if a closed curve surrounding Ω_1 is destroyed then the normal at the critical point is downward pointing. For, closed curves surrounding Ω_2 the opposite is true; i.e. when a closed curve is created then at the critical point the normal points downward. Thus, since the level sets at h and $-h$ are intervals, one sees that the normal points up as much as it points down. That is, g has as many zeros as poles.

We now drop the restrictions on the poles and zeros of g . Beyond these assumptions the argument above used only that $C_{h,R}$ was minimal and that the boundary curves γ_i ($i = 1, 2$) strictly spiral. It is not hard to check that these last two conditions

* (a) Initial orientation chosen at height $x_3 = h$. (b) A curve pinching off from Ω_1 . (c) Two curves pinching from one. (d) A curve pinching off from Ω_2

are preserved by small rotations around lines in the x_1 - x_2 plane. We claim that such rotations also ensure that the Gauss map of the new surface must have simple poles or zeros and these are on distinct level sets. To that end we let $C_{h,R}^\epsilon$ be the rotation of $C_{h,R}$ by ϵ degrees around a fixed line ℓ in the x_1 - x_2 plane and through the origin (note we do not rotate the ambient \mathbb{R}^3). Denote by Φ_ϵ the induced isometric isomorphism between the sets.

The strict spiraling of γ_1, γ_2 implies there exists an $\epsilon_0 > 0$, depending on α and R and a constant $K > 0$, depending on R so: for all $0 < \epsilon < \epsilon_0$, if $c \in (-h + K\epsilon, h - K\epsilon)$ then $\{x_3 = c\} \cap C_{h,R}^\epsilon$ meets $\partial C_{h,R}^\epsilon$ in two points. Moreover, by a suitable choice of ℓ the critical points will be on distinct level sets. Denote by g_ϵ the stereographic projection of the Gauss map of $C_{h,R}^\epsilon$. We now use the fact that g is meromorphic on Σ (and thus the zeros and poles of g are isolated) and that g_ϵ is obtained from g by a Möbius transform. Indeed, these two facts imply that (after shrinking ϵ_0) for $\epsilon \in (0, \epsilon_0)$, g_ϵ has only simple zeros and poles on $C_{h,R}^\epsilon$ and by our choice of ℓ these are on distinct levels of x_3 . By further shrinking ϵ_0 one can ensure that all of the critical values occur in the range $(-h + K\epsilon, h - K\epsilon)$. Thus, the level sets in $C_{h,R}^\epsilon$ of x_3 for $c \in (-h + K\epsilon, h - K\epsilon)$ consist of an interval with endpoints in $\partial C_{h,R}^\epsilon$, one in each γ_i for $i = 1, 2$, and the union of a finite number of closed curves.

Our original argument then immediately implies that g_ϵ has as many zeros as poles. Thus, $\int_{\partial C_{h,R}^\epsilon} \Phi_\epsilon^* \frac{dg_\epsilon}{g_\epsilon} = \int_{\partial C_{h,R}^\epsilon} \frac{dg_\epsilon}{g_\epsilon} = 0$ for $\epsilon < \epsilon_0$. Hence, as $\Phi_\epsilon^* \frac{dg_\epsilon}{g_\epsilon}$ is continuous in ϵ , $\int_{\partial C_{h,R}} \frac{dg}{g} = 0$. □

Corollary 4.2.3. *A holomorphic function $f : \Gamma \rightarrow \mathbb{C}$ exists so $e^f = g$ on Γ .*

4.2.2 Concluding properness of z

The strict spiraling in \mathcal{R}_S was used in Chapter 3 to show that the map $f = f_1 + if_2$ was, away from a neighborhood of the axis, a proper conformal diffeomorphism onto the union of two disjoint closed half-spaces. Since every level set of x_3 has an end in each of these sets, properness of z was then a consequence of Schwarz reflection and the Liouville theorem. The same is true when there is non-zero genus:

Proposition 4.2.4. *There exists a $\gamma_0 > 0$ so: with $\Omega_{\pm} = \{x \in \Gamma : \pm f_1(x) \geq \gamma_0\}$, f is a proper conformal diffeomorphism from Ω_{\pm} onto $\{z : \pm \operatorname{Re} z \geq \gamma_0\}$.*

Proof. Pick γ_0 as in Proposition 3.4.1 of Chapter 3 (where γ_0 depends only on the ϵ_0 of Theorem 1.2.1). As long as $f_1^{-1}(\gamma_0) \cap \partial\Gamma = \emptyset$, the proof in Chapter 3 carries over unchanged. Note, the structure of that proof only depends on having a lower bound for γ_0 and so we may increase γ_0 (if necessary) so $\gamma_0 > \max_{\partial\mathcal{R}_G} |f_1|$. \square

4.2.3 Conformal Structure of Σ

Proof. (Theorem 1.1.4) Coupled with the above results, the proof of Proposition 3.4.2 of Chapter 3 then gives that $z \rightarrow \pm\infty$ along each level set of x_3 ; that is $z : \Gamma \rightarrow \mathbb{C}$ is a proper holomorphic coordinate. Thus, $z(\Gamma)$ contains \mathbb{C} with a closed disk removed; in particular, Γ is conformally a punctured disk. Then, since $f_1^{-1}(\gamma_0) \cap \Gamma$ is a single smooth curve, f has a simple pole at the puncture. Similarly, by Proposition 1.2.3, z has a simple pole at the puncture. In Γ , the height differential $dh = dz$ and $\frac{dg}{g} = df$. \square

Embeddedness and the Weierstrass representation, (2.10), then imply Corollary 1.1.6:

Proof. Theorem 1.1.4 gives that, in Γ , $f(p) = \alpha z(p) + \beta + F(p)$ where $\alpha, \beta \in \mathbb{C}$ and $F : \Gamma \rightarrow \mathbb{C}$ is holomorphic and has holomorphic extension to the puncture (and has a zero there). By translating Σ parallel to the x_3 -axis and re-basing x_3^* we may assume $\beta = 0$. By Proposition 1.2.3, $\{x_3 = 0\} \cap \Gamma$ can be written as the union of two smooth proper curves, σ^\pm , each with one end in $\partial\Gamma$, and parametrized so $x_3^*(\sigma^\pm(t)) = t$ for $\pm t > T$; here $T > 0$ is large enough that $\sigma^\pm(t) \subset \mathcal{R}_S$. Let us denote by $\rho^\pm(t)$ and $\theta^\pm(t)$ the polar coordinates of $\sigma^\pm(t)$. Notice that as we are in Γ , $\text{Im } f(\sigma^\pm(t)) = (\text{Re } \alpha)t + \text{Im } F(\sigma^\pm(t))$. By the strict spiraling in \mathcal{R}_S , there are integers N^\pm so $|\theta^\pm(t) - \text{Im } f(\sigma^\pm(t))| < \pi N^\pm$ (see the proof of Proposition 3.4.1 of Chapter 3). Thus, since $F(\sigma^\pm(t)) \rightarrow 0$ as $|t| \rightarrow \infty$, if $\text{Re } \alpha \neq 0$ then $\theta^\pm(t)$ is unbounded as $|t|$ increases. That is, σ^+ and σ^- spiral infinitely and in opposite directions. Moreover, the strict spiraling also gives that $\rho^\pm(t)$ is strictly increasing in $|t|$. To see this note that since $\rho'(t)u_\rho(\rho(t), \theta(t)) + \theta'(t)u_\theta(\rho(t), \theta(t)) = 0$ along $\sigma^\pm(t)$ and $u_\theta \neq 0$, $\rho'(t)$ can only vanish when $\theta'(t)$ does. But, our choice of parametrization rules out the simultaneous vanishing of these two derivatives. This contradicts embeddedness, as such curves must eventually intersect. This last fact is most easily seen by looking at the universal cover of the annulus $\{\max\{\rho^\pm(\pm T_0)\} \leq \rho \leq \min\{\rho^\pm(\pm(T_0 + T_1))\}\}$ where $T_0, T_1 > T > 0$ are chosen so $|\theta^\pm(\pm(T_0 + T_1)) - \theta^\pm(\pm T_0)| \geq 4\pi$ and the annulus is non-empty. In particular, by appropriately lifting σ_+ and σ_- , the intersection is immediate. Therefore, $\text{Re } \alpha = 0$. □

Chapter 5

Local Results on Minimal Disks

Recall, for $\Sigma \subset \mathbb{R}^3$ a minimal disk, we say $(y, s) \in \Sigma \times \mathbb{R}^+$ is a (C) *blow-up pair* if $\sup_{B_s(y) \cap \Sigma} |A_\Sigma|^2 \leq 4C^2 s^{-2} = 4|A_\Sigma|^2(y)$ (here C is large and fixed). For Σ minimal with $\partial\Sigma \subset \partial B_R = \partial B_R(0)$ where $(0, s)$ is a blow-up pair, there are two important scales; R the outer scale and s the blow-up scale. The work of Colding and Minicozzi gives a value $0 < \Omega < 1$ so that the component of $\Sigma \cap B_{\Omega R}$ containing 0 consists of two multi-valued graphs glued together (see for instance Lemma 2.5 of [13] for a self-contained explanation). Sharpening this result, Theorem 5.1.2 below shows that on the scale of s (provided R/s is large), Σ is bi-Lipschitz to a piece of a helicoid with Lipschitz constant near 1. Using the surfaces constructed in [7] (which are the most distorted currently known) we show, in Theorem 5.2.1, that such a result cannot hold on the outer scale and indeed fails to hold on certain smaller scales.

5.1 Minimal Disks Close to a Helicoid

To prove Theorem 5.1.2, we first need to prove a technical lemma. Consider two surfaces $\Sigma_1, \Sigma_2 \subset \mathbb{R}^3$, so that Σ_2 is the graph of ν over Σ_1 . Then the map $\phi : \Sigma_1 \rightarrow \Sigma_2$ defined as $\phi(x) = x + \nu(x)\mathbf{n}(x)$ is smooth. Moreover, if ν is small in a C^1 sense, ϕ is an “almost isometry”.

Lemma 5.1.1. *Let Σ_2 be the graph of ν over Σ_1 , with $\Sigma_1 \subset B_R$, $\partial\Sigma_1 \subset \partial B_R$ and $|A_{\Sigma_1}| \leq 1$. Then, for ϵ sufficiently small, $|\nu| + |\nabla_{\Sigma_1}\nu| \leq \epsilon$ implies ϕ is a diffeomorphism with $1 - \epsilon \leq \|d\phi\| \leq 1 + \epsilon$.*

Proof. For ϵ sufficiently small (depending on Σ_1), ϕ is injective. Working in \mathbb{R}^3 , given orthonormal vectors $e_1, e_2 \in T_p\Sigma_1$ we compute:

$$(5.1) \quad d\phi_p(e_i) = e_i + \langle \nabla_{\Sigma_1}\nu(p), e_i \rangle \mathbf{n}(p) + \nu(p)D\mathbf{n}_p(e_i).$$

The last two terms are together controlled by ϵ . Hence, $1 - \epsilon < |d\phi_p(e_i)| < 1 + \epsilon$. \square

The local result will follow from a compactness argument (compare with Proposition 2 of [26]):

Theorem 5.1.2. *Given $\epsilon, R > 0$ there exists $R' \geq R$ so: Suppose $0 \in \Sigma'$ is an embedded minimal disk with $\Sigma' \subset B_{R's}(0)$, $\partial\Sigma' \subset \partial B_{R's}(0)$, and $(0, s)$ a blow-up pair. Then there exists Ω , a subset of a helicoid, so that Σ , the component of $\Sigma' \cap B_{Rs}$ containing 0 , is bi-Lipschitz with Ω , and the Lipschitz constant is in $(1 - \epsilon, 1 + \epsilon)$.*

Proof. By rescaling we may assume that $s = 1$. We proceed by contradiction. Suppose

no such R' existed for fixed ϵ, R . That is, there exists a sequence of counter-examples; embedded minimal disks $\Sigma'_i \subset B_{R_i}$, $\partial\Sigma'_i \subset \partial B_{R_i}$, $(0, 1)$ a C blow-up pair of each Σ'_i and $R \leq R_i \rightarrow \infty$, but Σ_i , the component of $B_R \cap \Sigma'_i$ containing zero, not close to a helicoid.

By definition, $|A_{\Sigma'_i}(0)|^2 = C > 0$ for all Σ'_i and so the lamination theory of Colding and Minicozzi implies that a subsequence of the Σ'_i converge smoothly and with multiplicity one to Σ_∞ , a complete embedded minimal disk. Namely, in any ball centered at 0 the curvature of Σ_i is uniformly bounded by Lemma 2.26 of [13]. Furthermore, the chord-arc bounds of [13] give uniform area bounds and so by standard compactness arguments one has smooth convergence (possibly with multiplicity) to Σ_∞ . If the multiplicity of the convergence is greater than 1, then one can construct a positive solution to the Jacobi equation (see Appendix B of [4]). That implies Σ_∞ is stable, and thus a plane by the Bernstein theorem, contradicting the curvature at 0. As Corollary 0.7 of [13] gives properness of Σ_∞ , Theorem 3.0.2 implies Σ_∞ is a helicoid. We may, by rescaling, assume Σ_∞ has curvature 1 along the axis.

For any fixed R' a subsequence of $\Sigma'_i \cap B_{R'}$ converges to $\Sigma_\infty \cap B_{R'}$ in the smooth topology. And so, for any ϵ , with i sufficiently large, we find a smooth ν_i defined on a subset of Σ_∞ so that $|\nu_i| + |\nabla_{\Sigma_\infty} \nu_i| < \epsilon$ and the graph of ν_i is $\Sigma'_i \cap B_{R'}$. Choosing R' large enough to ensure minimizing geodesics between points in Σ_i lie in $\Sigma'_i \cap B_{R'}$ (using the chord-arc bounds of [13]), Lemma 5.1.1 gives the desired contradiction. \square

5.2 Distortions of the Helicoid

Recall that as an application of their work on the structure of disks, Colding and Minicozzi proved a compactness result for sequences of embedded minimal disks $0 \in \Sigma_i \subset \mathbb{R}^3$ as long as $\partial\Sigma_i \subset \partial B_{R_i}$ and $R_i \rightarrow \infty$. In particular, they show there are only two options. Either such a sequence contains a subsequence converging smoothly on compact sets to a complete embedded minimal disk or, if the curvature is unbounded in some compact subset of \mathbb{R}^3 , the convergence is (in a certain sense, see [12] for details) to a singular minimal lamination of parallel planes. The surfaces constructed by Colding and Minicozzi in [7] show that the condition that the boundaries of the surface go to infinity is essential, i.e this compactness result is global in nature. (Figure 5.1 shows a cross section of one of Colding and Minicozzi's examples, which represent extreme distortions of helicoids. We indicate the two important scales: $R = 1$ the outer scale and s the blow-up scale. Here $(0, s)$ is a blow-up pair.)

In a similar vein, the result depends very strongly on the ambient geometry of the three-manifold. In particular, in the proof of their compactness result, Colding and Minicozzi rely heavily on a flux argument (the details of which are in [6]). That is they use that the coordinate functions of \mathbb{R}^3 restrict to harmonic functions on minimal $\Sigma \subset \mathbb{R}^3$, a fact that generalizes only to certain other highly symmetric three-manifolds.

One of the most important problems in this area is determining when a Colding and Minicozzi type of compactness result (or indeed any compactness result) extends to surfaces embedded in more arbitrary three-manifolds. Understanding precisely the best scale for which the Lipschitz approximation holds (for which Theorem 5.2.1

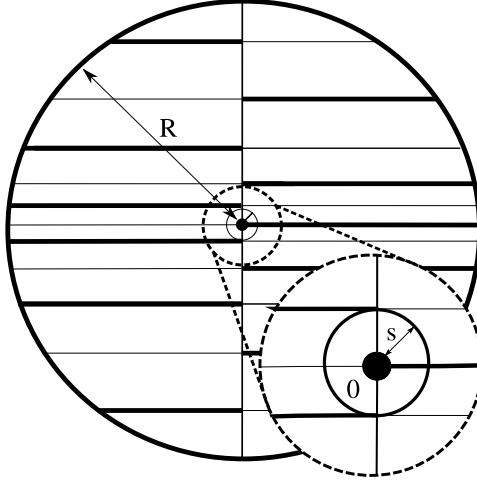


Figure 5.1: Colding-Minicozzi distorted helicoids

gives an upper bound) may be an important tool to establish removable singularities theorems for minimal laminations in arbitrary Riemannian manifolds. In turn, such results could prove key to proving more general compactness theorems.

Theorem 5.2.1. *Given $1 > \Omega, \epsilon > 0$ and $1/2 > \gamma \geq 0$ there exists an embedded minimal disk $0 \in \Sigma$ with $\partial\Sigma \subset \partial B_R$ and $(0, s)$ a blow-up pair so: the component of $B_{\Omega R^{1-\gamma s^\gamma}} \cap \Sigma$ containing 0 is not bi-Lipschitz to a piece of a helicoid with Lipschitz constant in $((1 + \epsilon)^{-1}, 1 + \epsilon)$.*

To produce our example, we first recall the surfaces constructed in [7]:

Theorem 5.2.2. *(Theorem 1 of [7]) There is a sequence of compact embedded minimal disks $0 \in \Sigma_i \subset B_1 \subset \mathbb{R}^3$ with $\partial\Sigma_i \subset \partial B_1$ containing the vertical segment $\{(0, 0, t) : |t| \leq 1\} \subset \Sigma_i$ such that the following conditions are satisfied:*

1. $\lim_{i \rightarrow \infty} |A_{\Sigma_i}|^2(0) \rightarrow \infty$
2. $\sup_{\Sigma_i} |A_{\Sigma_i}|^2 \leq 4|A_{\Sigma_i}|^2(0) = 8a_i^{-4}$ for a sequence $a_i \rightarrow 0$

3. $\sup_i \sup_{\Sigma_i \setminus B_\delta} |A_{\Sigma_i}|^2 < K\delta^{-4}$ for all $1 > \delta > 0$ and K a universal constant.

4. $\Sigma_i \setminus \{x_3 - \text{axis}\} = \Sigma_{1,i} \cup \Sigma_{2,i}$ for multi-valued graphs $\Sigma_{1,i}$ and $\Sigma_{2,i}$.

Remark 5.2.3. (2) and (3) are slightly sharper than what is stated in Theorem 1 of [7], but follow easily. (2) follows from the Weierstrass data (see Equation (2.3) of [7]). This also gives (3) near the axis, whereas away from the axis use (4) and Heinz's curvature estimates.

Next introduce some notation. For a surface Σ (with a smooth metric) we denote intrinsic balls of radius s , centered at p , by $\mathcal{B}_s^\Sigma(p)$ and define the (*intrinsic*) *density ratio* at a point p as: $\theta_s(p, \Sigma) = (\pi s^2)^{-1} \text{Area}(\mathcal{B}_s^\Sigma(p))$. When Σ is immersed in \mathbb{R}^3 and has the induced metric, $\theta_s(p, \Sigma) \leq \Theta_s(p, \Sigma) = (\pi s^2)^{-1} \text{Area}(B_s(p) \cap \Sigma)$, the usual (*extrinsic*) density ratio. Importantly, the intrinsic density ratio is well-behaved under bi-Lipschitz maps. Indeed, if $f : \Sigma \rightarrow \Sigma'$ is injective and with $\alpha^{-1} < \text{Lip } f < \alpha$ (where $\text{Lip } f$ is the Lipschitz constant of f), then:

$$(5.2) \quad \alpha^{-4} \theta_{\alpha^{-1}s}(p, \Sigma) \leq \theta_s(f(p), \Sigma') \leq \alpha^4 \theta_{\alpha s}(p, \Sigma).$$

This follows from the inclusion, $\mathcal{B}_{\alpha^{-1}s}^\Sigma(f^{-1}(p)) \subset f^{-1}(\mathcal{B}_s^{\Sigma'}(p))$ and the behavior of area under Lipschitz maps, $\text{Area}(f^{-1}(\mathcal{B}_s^{\Sigma'}(p))) \leq (\text{Lip } f^{-1})^2 \text{Area}(\mathcal{B}_s^{\Sigma'}(p))$.

Note that by standard area estimates for minimal graphs, if $\Sigma \cap B_s(p)$ is a minimal graph then $\theta_s(p, \Sigma) \leq 2$. In contrast, for a point near the axis of a helicoid, for large s the density ratio is large. Thus, in a helicoid the density ratio for a fixed, large s measures, in a rough sense, the distance to the axis. More generally, this holds near

blow-up pairs of embedded minimal disks:

Lemma 5.2.4. *Given $D > 0$ there exists $R > 1$ so: If $0 \in \Sigma \subset B_{2Rs}$ is an embedded minimal disk with $\partial\Sigma \subset \partial B_{2Rs}$ and $(0, s)$ a blow-up pair then $\theta_{Rs}(0, \Sigma) \geq D$.*

Proof. We proceed by contradiction, that is suppose there were a $D > 0$ and embedded minimal disks $0 \in \Sigma_i$ with $\partial\Sigma_i \subset \partial B_{2R_i s}$ with $R_i \rightarrow \infty$ and $(0, s)$ a blow-up pair so that $\theta_{R_i s}(0, \Sigma_i) \leq D$. The chord-arc bounds of [13] imply there is a $1 > \gamma > 0$ so $\mathcal{B}_{R_i s}^{\Sigma_i}(0) \supset \Sigma_i \cap B_{\gamma R_i s}$. Hence, the intrinsic density ratio bounds the extrinsic density ratio, i.e. $D \geq \theta_{R_i s}(p, \Sigma_i) \geq \gamma^2 \Theta_{\gamma R_i s}(p, \Sigma_i)$. Then, by a result of Schoen and Simon [31] there is a constant $K = K(D\gamma^{-2})$, so $|A_{\Sigma_i}|^2(0) \leq K(\gamma R_i s)^{-2}$. For R_i large this contradicts that $(0, s)$ is a blow-up pair for all Σ_i . \square

Remark 5.2.5. Note that the above does not depend on the strength of chord-arc bounds. In fact, it is also an immediate consequence of the fact that intrinsic area bounds on a disk give total curvature bounds. In turn, the total curvature bounds again yield uniform curvature bounds. See Section 1 of [10] for more detail.

In order to show the existence of the surface Σ of Theorem 5.2.1, we exploit the fact that two points on a helicoid that are equally far from the axis must have the same density ratio. Assuming the existence of a Lipschitz map between Σ and a helicoid, we get a contradiction by comparing the densities for two appropriately chosen points that map to points equally far from the axis of the helicoid.

Proof. (of Theorem 5.2.1) Fix $1 > \Omega, \epsilon > 0$ and $1/2 > \gamma \geq 0$ and set $\alpha = 1 + \epsilon$. Let Σ_i be the surfaces of Theorem 5.2.2; we claim for i large, Σ_i will be the desired

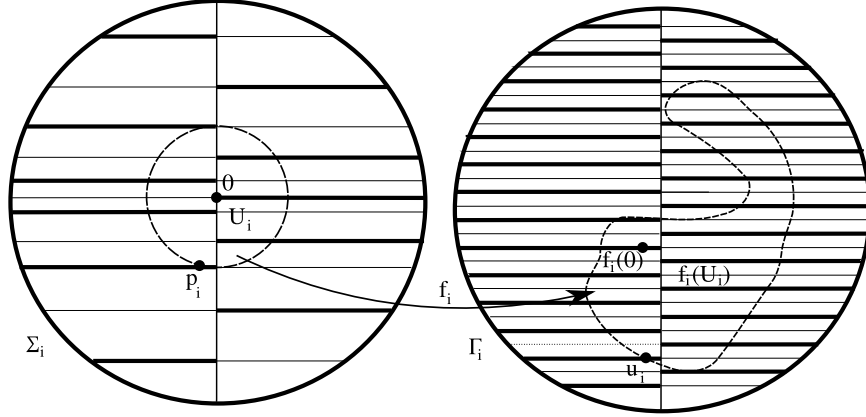


Figure 5.2: The points p_i and u_i

example. Suppose this was not the case. Setting $s_i = Ca_i^2/\sqrt{2}$, where a_i is as in (2) and C is the blow-up constant, one has $(0, s_i)$ is a blow-up pair in Σ_i , since $\sup_{\Sigma_i \cap B_{s_i}} |A_{\Sigma_i}|^2 \leq 8a_i^{-4} = 4C^2 s_i^{-2} = 4|A_{\Sigma_i}|^2(0)$, moreover, $s_i \rightarrow 0$. Hence, with $R_i = \Omega s_i^\gamma < 1$, the component of $B_{R_i} \cap \Sigma_i$ containing 0 , Σ'_i , is bi-Lipschitz to a piece of a helicoid with Lipschitz constant in (α^{-1}, α) . That is, there are subsets Γ_i of helicoids and diffeomorphisms $f_i : \Sigma'_i \rightarrow \Gamma_i$ with $\text{Lip } f_i \in (\alpha^{-1}, \alpha)$.

We now begin the density comparison. First, Lemma 5.2.4 implies there is a constant $r > 0$ so for i large $\theta_{rs_i}(0, \Sigma'_i) \geq 4\alpha^8$ and thus by (5.2) $\theta_{\alpha rs_i}(f_i(0), \Gamma_i) \geq 4\alpha^4$. We proceed to find a point with small density on Σ_i that maps to a point on Γ_i equally far from the axis as $f_i(0)$ (which has large density). Let U_i be the (interior) of the component of $B_{1/2R_i} \cap \Sigma_i$ containing 0 . Note for i large enough, as $s_i/R_i \rightarrow 0$, the distance between ∂U_i and $\partial \Sigma'_i$ is greater than $4\alpha^2 rs_i$. Similarly, for $p \in \partial U_i$ for i large, $p' \in \mathcal{B}_{4\alpha^2 rs_i}^{\Sigma'_i}(p)$ implies $|p'| \geq \frac{1}{4}R_i$. Hence, property (3) gives that $|A_{\Sigma'_i}|^2(p') \leq K' s_i^{-4\gamma}$. Thus, for i sufficiently large $\mathcal{B}_{\alpha^2 rs_i}(p)$ is a graph and so $\theta_{\alpha^2 rs_i}(p, \Sigma'_i) \leq 2$. Pick $u_i \in \partial f(U_i)$ at the same distance to the axis as $f_i(0)$ and so

the density ratio is the same at both points. (See Figure 5.2. Note that the density ratio of u_i is much larger than the density ratio of p_i .) As $f_i(U_i)$ is an open subset of Γ_i containing $f_i(0)$, $p_i = f_i^{-1}(u_i) \in \partial U_i$. Notice that $\theta_{\alpha r s_i}(u_i, \Gamma_i) = \theta_{\alpha r s_i}(f_i(0), \Gamma_i) \geq 4\alpha^4$ so $2\alpha^4 \geq \alpha^4 \theta_{\alpha^2 r s_i}(p_i, \Sigma'_i) \geq 4\alpha^4$.

□

Bibliography

- [1] J. Bernstein and C. Breiner. Conformal structure of minimal surfaces with finite topology. *Preprint*.
- [2] J. Bernstein and C. Breiner. Helicoid-like minimal disks and uniqueness. *Preprint*.
- [3] J. Bernstein and C. Breiner. Distortions of the helicoid. *Geometriae Dedicata*, 137(1):143–147, 2008.
- [4] T. H. Colding and W. P. Minicozzi II. The Space of Embedded Minimal Surfaces of Fixed Genus in a 3-manifold V; Fixed Genus. *Preprint*.
- [5] T. H. Colding and W. P. Minicozzi II. *Minimal Surfaces, Courant Lecture Notes in Math.*, 4. New York University, Courant Institute of Math. Sciences, New York, 1999.
- [6] T. H. Colding and W. P. Minicozzi II. Multivalued minimal graphs and properness of disks. *Int. Math. Res. Not.*, (21):1111–1127, 2002.

- [7] T. H. Colding and W. P. Minicozzi II. Embedded minimal disks: Proper versus nonproper - global versus local. *Trans. of the AMS*, 356:283–289, 2004.
- [8] T. H. Colding and W. P. Minicozzi II. An excursion into geometric analysis. *Surv. in Diff. Geom.*, IX:83–146, 2004.
- [9] T. H. Colding and W. P. Minicozzi II. The space of embedded minimal surfaces of fixed genus in a 3-manifold I; Estimates off the axis for disks. *Ann. of Math. (2)*, 160(1):27–68, 2004.
- [10] T. H. Colding and W. P. Minicozzi II. The space of embedded minimal surfaces of fixed genus in a 3-manifold II; Multi-valued graphs in disks. *Ann. of Math. (2)*, 160(1):69–92, 2004.
- [11] T. H. Colding and W. P. Minicozzi II. The space of embedded minimal surfaces of fixed genus in a 3-manifold III; Planar domains. *Ann. of Math. (2)*, 160(2):523–572, 2004.
- [12] T. H. Colding and W. P. Minicozzi II. The space of embedded minimal surfaces of fixed genus in a 3-manifold IV; Locally simply connected. *Ann. of Math. (2)*, 160(2):573–615, 2004.
- [13] T. H. Colding and W. P. Minicozzi II. The Calabi-Yau conjectures for embedded surfaces. *Ann. of Math.*, 167(1):211–243, 2008.
- [14] P. Collin. Topologie et courbure des surfaces minimales proprement plongees de \mathbb{R}^3 . *Ann. of Math.*, 145:1–31, 1997.

- [15] P. Collin, R. Kusner, W. H. Meeks III, and H. Rosenberg. The topology, geometry and conformal structure of properly embedded minimal surfaces. *J. Differential Geom.*, 67(2):377–393, 2004.
- [16] M. do Carmo and C.K. Peng. Stable complete minimal surfaces in \mathbb{R}^3 are planes. *Bulletin of the AMS*, 1(6):903–906, 1979.
- [17] D. Fischer-Colbrie and R. Schoen. The structure of complete stable minimal surfaces in 3-manifolds of nonnegative scalar curvature. *Comm. Pure Appl. Math.*, 33:199–211, 1980.
- [18] D. Gilbarg and N. S. Trudinger. *Elliptic Partial Differential Equations of Second Order*. Springer-Verlag, 1998.
- [19] L. Hauswirth, J. Perez, and P. Romon. Embedded minimal ends of finite type. *Trans. AMS*, 353(4):1335–1370, 2001.
- [20] D. Hoffman, H. Karcher, and F. Wei. *Global Analysis in Modern Mathematics*, chapter The Genus One Helicoid and the Minimal Surfaces that Led to its Discovery. Publish or Perish, 1993.
- [21] D. Hoffman, M. Weber, and M. Wolf. The genus-one helicoid as a limit of screw-motion invariant helicoids with handles. *Clay Math. Proc., Global Theory of Minimal Surfaces*, 2:243–258, 2001.
- [22] D. Hoffman, M. Weber, and M. Wolf. An embedded genus-one helicoid. *Annals of Math.*, 169(2):347–448, 2009.

- [23] D. Hoffman and F. Wei. Construction of a helicoid with handle. *Preprint*.
- [24] D. Hoffman and B. White. The geometry of genus-one helicoids. *Comm. Math. Helv.* To Appear.
- [25] D. Hoffman and B. White. Genus-one helicoids from a variational point of view. *Comm. Math. Helv.*, 83(4):767–813, 2008.
- [26] W. H. Meeks III. Regularity of the singular set in the Colding-Minicozzi lamination theorem. *Duke Math. J.*, 123(2):329–334, 2004.
- [27] W. H. Meeks III and H. Rosenberg. The uniqueness of the helicoid. *Ann. of Math. (2)*, 161(2):727–758, 2005.
- [28] W.H. Meeks III and H. Rosenberg. The geometry and conformal structure of properly embedded minimal surfaces of finite topology in \mathbb{R}^3 . *Invent. Math.*, 114(3):625–639, 1993.
- [29] W. H. Meeks and M. Weber. Bending the helicoid. *Mathematische Annalen*, 339(4):783–798, 2007.
- [30] R. Osserman. *A survey of minimal surfaces*. Dover Publications, 1986.
- [31] R. Schoen and L. Simon. *Seminar on minimal submanifolds*, *Ann. of Math. Studies*, chapter Regularity of simply connected surfaces with quasiconformal Gauss map. Princeton University Press, 1983.
- [32] M. Weber, D. Hoffman, and M. Wolf. An embedded genus-one helicoid. *PNAS*, 102(46):16566–16568, 2005.

Curriculum Vitae

Christine Breiner was born in Columbus, Ohio, on July 27, 1977. She received her Bachelor's Degree in mathematics from Kenyon College in Gambier, Ohio, in May of 1999. She also received a Master's degree in mathematics from Johns Hopkins University in May of 2005. Christine defended this dissertation on March 12, 2009.